12 *Mechanical Properties*

12.1 General Introduction

Many years elapsed after the work of Davenport and Bain before the commercial exploitation of bainitic steels. There were difficulties in obtaining fully bainitic microstructures in sizable samples of steel. It has long been recognised that the influence of bainite on the mechanical behaviour of a steel is difficult to understand because of the inability to attain fully bainitic microstructures at all transformation temperatures, a consequence of the incomplete reaction phenomenon (Hehemann *et al.*, 1957). Isothermal transformation to bainite was considered impractical on a commercial scale, continuous cooling being the preferred heat treatment. Furthermore, continuous cooling at a rate greater than $\simeq 50\,\mathrm{K\,s^{-1}}$ during transformation was also believed impractical. In these circumstances, lean steels gave mixed microstructures of allotriomorphic ferrite and bainite, whereas richly alloyed steels transformed only partly to bainite, the remaining microstructure consisting of martensite and retained austenite. It was not until low-alloy, low-carbon steels, containing small amounts of boron and molybdenum to suppress proeutectoid ferrite were developed that the potential for commercial exploitation became realistic (Irvine and Pickering, 1957).

Boron is effective in retarding proeutectoid ferrite formation but has a negligible effect on the bainite reaction, allowing bainitic microstructures to be obtained over a wider range of cooling rates. The segregation of boron to the austenite grain boundaries leads to a reduction in their energy, thereby making them less favourable as sites for the heterogeneous nucleation of ferrite. The reason why the effect is more pronounced for allotriomorphic ferrite than for bainite has not been investigated, but it may be associated with the fact that for bainite, which grows in the form of sheaves of small platelets, the vast majority of platelets nucleate autocatalytically after the initial formation of some platelets at the austenite grain boundaries (Chapter 6). Boron thus increases the bainite hardenability. The level of other alloying additions can, in the presence of boron, be kept low enough to avoid the formation of martensite. Steels of typical composition Fe–0.0033B–0.52Mn–0.54Mo–0.11Si–0.10C, wt% were found to yield fully bainitic microstructures with very little martensite during

normalising (i.e. air cooling from the austenitising temperature), and permitted the characterisation of the mechanical properties of bainite in isolation.

Many investigations of the mechanical properties fail to recognise that the microstructures studied were not fully bainitic. In the discussion that follows, attention is restricted to cases where the microstructure has been characterised thoroughly, and where it plays a significant role in determining the mechanical properties.

12.2 The Strength of Bainite

The strength of bainite can in principle be factorised into components consisting of the intrinsic strength of pure annealed iron (σ_{Fe}), substitutional solid solution strengthening contributions (σ_{SS}), strengthening due to carbon in solid solution (σ_C), and a variety of microstructural components including dislocation strengthening, particle effects and grain size effects. Thus,

$$\sigma = \sigma_{Fe} + \sum_i \sigma_{SS}^i + \sigma_C + k_\epsilon(\overline{L}_3)^{-1} + k_P\Delta^{-1} + C_{10}\rho_d^{0.5} \qquad (12.1)$$

where ρ_d is the dislocation density and Δ the average distance between a cementite particle and its two or three nearest neighbours. From measurements done on martensite, k_ϵ is approximately 115 MPa m; assuming that the cementite particles are spherical and of a uniform size, k_P is given approximately by $0.52\,V_\theta$ MPa m, where V_θ is the volume fraction of cementite (Daigne *et al.*, 1982). Dislocation theory for body-centred cubic metals gives $C_{10} = 0.38\,\mu b \simeq 7.34$ Pam (Keh and Weissmann, 1963). The carbon and substitutional solutes are listed separately because their solid solution strengthening contributions vary differently with concentration. For carbon, the strengthening varies with the square root of concentration (Speich and Warlimont, 1968; Christian, 1971), whereas for the substitutional solutes there is a direct relationship (Leslie, 1982). Equation 12.1 illustrates the form of the relationships, it is in practice difficult to decipher the microstructural contributions because parameters such as grain size and particle spacing cannot be varied independently. Figure 12.1 illustrates the magnitudes of the terms involved, together with some typical data for a fully bainitic microstructure.

12.2.1 Hardness

The hardness of bainite increases linearly with carbon concentration, by approximately 190 HV per wt% (Irvine and Pickering, 1965). This contrasts with a change of about 950 HV per wt% in the case of carbon-supersaturated martensite. The austenitising temperature does not influence the hardness unless it is not high enough to dissolve all the carbides (Irvine and

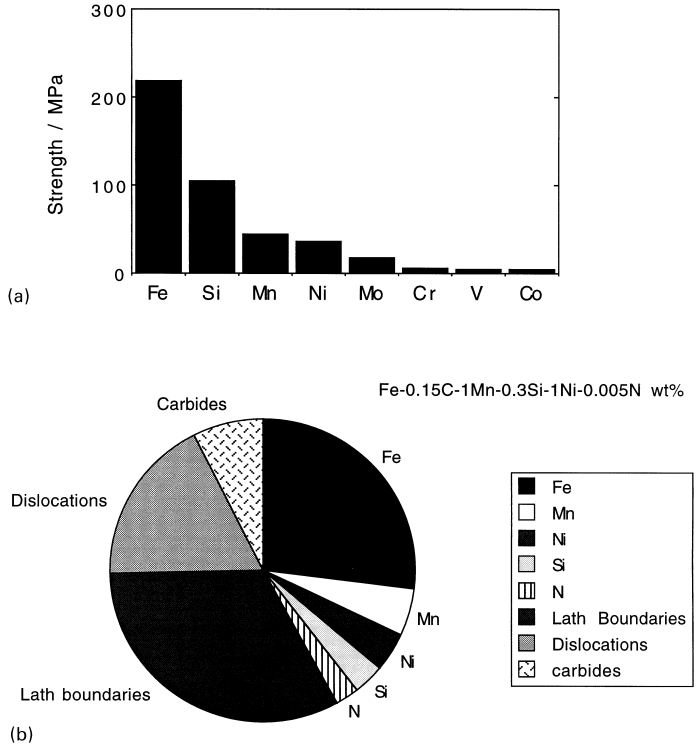

Fig. 12.1 The tensile yield strength of bainite at 25 °C and a strain rate of 0.0025 s^{-1}: (a) typical solid solution strengthening contributions per wt% of solute in ferrite; the intrinsic strength of pure iron is also included (data from Leslie, 1982); (b) estimated contributions to the strength of a fully bainitic sample.

Pickering, 1965). For mixed microstructures, the hardness depends on the transformation temperature and composition. This is because the stability of the residual austenite to martensitic transformation changes with its carbon concentration, the limiting value of which depends on the transformation temperature via the T_0' curve of the phase diagram.

Reconstructive transformations become incredibly slow below B_S in high-alloy steels. Hence, any austenite left untransformed during the bainite reaction either decomposes into untempered high-carbon martensite or is retained to ambient temperature. In low-alloy steels the residual austenite may transform into some form of degenerate pearlite. These secondary transformations have for a long time been known to influence the hardness of the microstructure. Lyman and Troiano (1946) found that for a series of Fe–Cr–C alloys the hardness for the 0.08 wt% C alloy was insensitive to the isothermal transformation temperature (Fig. 12.2). The low carbon concentration ensures that the

[13:37 3/9/01 C:/3B2 Templates/keith/3750 BAINITE.605/3750-012.3d] Ref: 0000 Auth: Title: Chapter 00 Page: 287 285-342

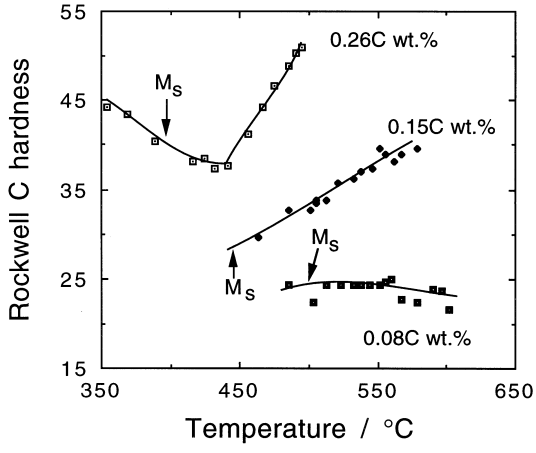

Fig. 12.2 Variation in hardness as a function of the isothermal transformation temperature (after Lyman and Troiano, 1946.)

microstructure is almost fully bainitic for all of the temperatures studied. This contrasts with higher carbon alloys, where the hardness first decreases as the transformation temperature is reduced; this is because the fraction of bainite increases at the expense of residual phases like martensite and degenerate pearlite.[†]

The *microhardness* of bainite, in a mixed microstructure of bainite and pearlite obtained by isothermal transformation, is found to be less than that of the pearlite, Fig. 12.3. This remains the case even when the pearlite and bainite have been generated at the same temperature. This behaviour is easy to explain once it is realised that the pearlite grows from *carbon-enriched* austenite and hence contains a much larger fraction of cementite than the bainite.

The hardness of bainite is insensitive to the austenite grain size, even though the latter influences the bainite sheaf thickness (Kamada *et al*., 1976). This is expected since the bainite sub-unit size is hardly influenced by the austenite grain size (Chapter 2). Since the sub-units are much smaller they exert an overriding influence on strength. For the same reason, the hardness of fully bainitic microstructures is not sensitive to the austenitising temperature (Irvine and Pickering, 1965; Kamada *et al*., 1976).

[†]This happens even though the dislocation density of bainitic ferrite increases as the transformation temperature decreases (Smith, 1984). The reduction in the quantity of hard phases (martensite, pearlite) compensates for the increase in dislocation density.

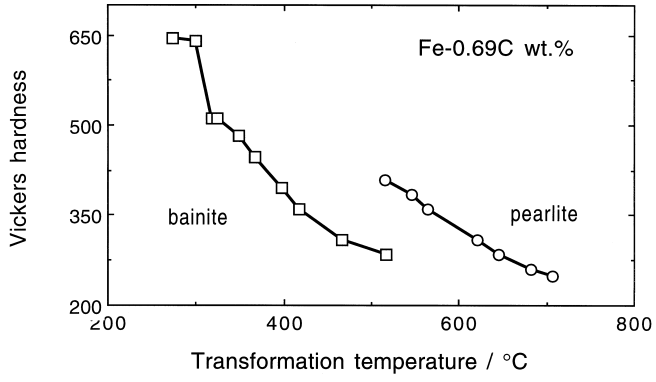

Fig. 12.3 Microhardness data from plain carbon steels transformed isothermally to a mixture of bainite and pearlite (after Ohmori and Honeycombe, 1971).

12.2.2 Tensile Strength

Although there is evidence that bainitic ferrite retains an excess concentration of carbon even after annealing (Bhadeshia and Waugh, 1981, 1982; Stark *et al.*, 1988), the majority of dislocations in bainite are believed to be mobile. Sharp yield points are not observed during tensile tests. The main effect of carbon on strength is through carbide precipitation. Cementite is the most common carbide; it precipitates in a coarse form without substantial coherency strains. Matrix dislocations have to bypass the cementite particles because they are unable to cut through them. It follows that the effect of carbon on the strength of bainite is rather small, approximately 400 MPa per 1 wt% of carbon (Irvine *et al.*, 1957).

Plates of bainitic ferrite are typically 10 μm in length and about 0.2 μm in thickness. This gives a small mean free path for dislocation glide because the probability of the slip parallel to the plate is small. The effective grain size of the plate is then about twice the plate thickness. There is only one other method, mechanical alloying (Benjamin, 1970), which can give a similarly small grain size in bulk materials. It is not surprising that the main microstructural contribution to the strength of bainite is from its fine grain size (Irvine *et al.*, 1957).

There have been many attempts at an analysis of the grain size contribution to the strength of bainite, most of them being based on the Hall–Petch relationship. This predicts a linear relationship between the strength and the reciprocal of the square root of the grain size. Although most data on bainite can be fitted to the Hall–Petch relation with $\sigma_y \propto (\overline{L})^{-1/2}$ (Siriwardene, 1955; Pickering, 1967), the results are difficult to interpret because the platelet size cannot be

[13:37 3/9/01 C:/3B2 Templates/keith/3750 BAINITE.605/3750-012.3d] Ref: 0000 Auth: Title: Chapter 00 Page: 289 285-342

altered without influencing other variables such as the dislocation density and the number density of carbide particles.

The Hall–Petch relationship relies on a description of macroscopic yielding in which a dislocation pile-up generates a large enough stress concentration to stimulate a dislocation source in an adjacent grain, thereby transmitting deformation across grains. If the grain size is large, then the number of dislocations that can participate in the pile-up increases. The larger stress field of the pile-up makes it easier to stimulate distant sources, thereby leading to a reduction in the yield strength.

This is an unlikely description of events when the grain size is fine. The slip plane dimensions become too small to allow the existence of pile-ups. Yielding is then determined by the stress necessary to expand a dislocation loop across a slip plane (Langford and Cohen, 1969, 1970, 1975). The yield stress in these circumstances varies as the inverse of the grain size, $\sigma_y \propto (\overline{L})^{-1}$. The strength of heavily cold-deformed iron and of martensitic samples has been interpreted using such a relationship (Langford and Cohen, 1969, 1970, 1975; Naylor, 1979; Daigne *et al.*, 1982). The changeover from the Hall–Petch to the Langford–Cohen relation should occur when the slip plane dimensions become $\simeq 1\mu m$.

An attempt has been made to separate the effect of bainite grain size and particle strengthening using multiple regression analysis (Gladman, 1972). The results indicate that carbides do not contribute much to the strength of bainite. This probably is a reasonable conclusion, but it has been pointed out that the analysis includes empirical constants which are difficult to justify (Honeycombe and Pickering, 1972).

12.2.3 Effect of Austenite Grain Size

We have seen already that the hardness of bainite is insensitive to the austenite grain structure. There have, nevertheless, been many investigations on the role of the austenite grain size and the bainite packet (sheaf) size on the strength. Both of these features are much coarser than the lath size which is probably the parameter with the greatest influence on flow stress. Published plots showing a Hall–Petch dependence of strength on austenite grain size or bainite packet size are probably fortuitous. Experiments have demonstrated that for martensite, the strength does not depend on the austenite grain size in low carbon steels (Brownrigg, 1973). Whether this applies to bainite depends on the effectiveness of the low-misorientation boundaries that exist between neighbouring platelets within a sheaf, in hindering dislocation motion. If there are films of austenite, or carbides separating the platelets within a sheaf, then they should be much more formidable barriers than implied by the small crystallographic misorientations between the sub-units. Since this is the case for most bainitic

steels, it is unlikely that the austenite grain size or the packet size have any significant effect on strength.

12.2.4 Effect of Tempering on Strength

The hardness and tensile strength of fully bainitic microstructures decrease during tempering, the rate of change being larger for lower bainite, which has a higher starting hardness. As might be expected, it is the highest strength steels which undergo the largest changes in strength during tempering (Bush and Kelly, 1971). After all, low-strength steels are not much stronger than the strength of the fully tempered microstructure.

The strength at any stage of tempering correlates well with the interparticle spacing, irrespective of the thermal history of the bainite (Deep and Williams, 1975). However, the grain size, particle size and distribution and dislocation density are not independent parameters. For example, studies using low carbon bainitic steels have established that the combined strengthening effects of dislocation density and the ultrafine bainitic ferrite grain size are substantial (McEvily and Magee, 1968). In bainitic steels containing retained austenite, the yield strength is found to be low due to the relative softness of the austenite. Tempering these steels at temperatures as high as 540 °C does not lead to a reduction in yield strength, the general softening of the microstructure being compensated by the removal of the soft austenite which decomposes diffusionally into a harder mixture of ferrite and carbides (Kalish *et al*., 1956).

There are interesting empirical relationships between strength and transformation characteristics, particularly for low carbon, low alloy, fully bainitic steels. Irvine *et al*. (1957) found a negative linear correlation between tensile strength and the 'temperature of maximum rate of transformation', indicating that the alloying element effect on strength can be rationalised simply on the basis of transformation kinetics (Fig. 12.4). For similar steels, the tensile strength is also found to correlate with the B_S temperature (Coldren *et al*., 1969). These results may be explained qualitatively: the bainite obtained at lower transformation temperatures should have a finer plate size and a larger dislocation density.

12.2.5 The Strength Differential Effect

Plastic deformation in metals becomes easier when the sense of the deformation is suddenly reversed. Thus, when the loading is changed from compression to tension (or vice versa), the deformation occurs more easily than would have been the case had it continued in the compressive mode. This is called the

[13:37 3/9/01 C:/3B2 Templates/keith/3750 BAINITE.605/3750-012.3d] Ref: 0000 Auth: Title: Chapter 00 Page: 291 285-342

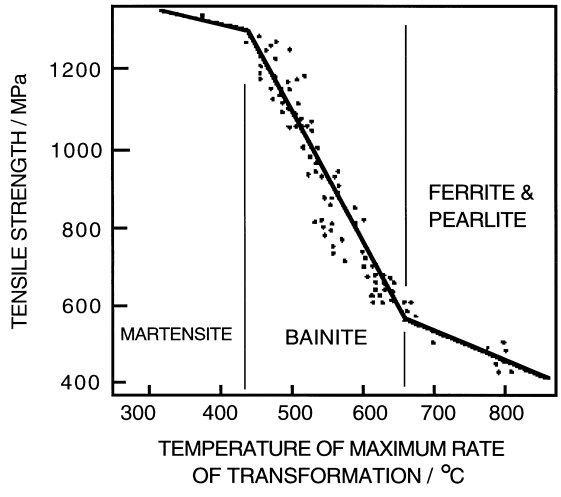

Fig. 12.4 Variation in the tensile strength of structural steels as a function of the temperature at which the rate of transformation is greatest during continuous cooling heat treatment (Irvine *et al*., 1957).

Bauschinger effect. A simple explanation is that deformation creates reversible features such as dislocation pile-ups, which relax and hence aid flow in the reverse direction when the sense of the load is changed. The effect therefore becomes less prominent as the total plastic strain increases, since the general build up in defect density makes it difficult for relaxation to occur.

Careful experiments on steels containing either martensite, bainite or Widmanstätten ferrite show that they have a higher yield stress in compression than in tension. This *strength differential effect* (Rauch and Leslie, 1972) persists even at large plastic strains, is independent of the starting sense of the deformation, and is not influenced by cyclic prestraining. It is believed to be associated with microstructures containing a high density of dislocations. It is not, for example, found in annealed ferrite or in ferrite–pearlite mixtures (Leslie, 1982). It has been shown to be inconsistent with an internally induced Bauschinger effect. Since the elastic modulus is similar in both tension and compression, the results cannot be explained in terms of the opening of microcracks during tension but not in compression (Rauch and Leslie, 1972).

There is no complete explanation for the phenomenon (Kennon, 1974), but it may be related to the presence of a nonlinear elastic interaction between dislocations and interstitial carbon atoms, the interaction being asymmetric in tension and compression (Hirth and Cohen, 1970). But it is not clear why the effect should be confined to microstructures with large dislocation densities.

12.2.6 Temperature Dependence of Strength

With the exception of creep-resistant alloys, most bainitic steels are used at ambient temperature. However, austempered ductile cast irons, which have a microstructure which is a mixture of graphite, bainitic ferrite, martensite and retained austenite, have found applications in automobile engines where the operating temperature might reach between 400–600 K. The strength of the iron hardly changes with temperature up to about 550 K; deformation is resisted by strain ageing due to interstitial carbon atoms in the bainitic ferrite (Shieh *et al*., 1993, 1995). Serrated stress–strain curves are observed during deformation at higher temperatures, consistent with the classical Portevin–Le Chatelier effect. Thus, the solute atoms are sufficiently mobile to migrate to moving dislocations, which then have to break away, the process repeating during the test. The serrations disappear at even higher temperatures where the carbon can diffuse fast enough to migrate with the dislocation.

12.3 Ratio of Proof Stress to Ultimate Tensile Strength

If a material does not exhibit a sharp yield point, then it is necessary to define a proof stress which is the stress needed to produce a specified amount of plastic strain (usually 0.2%). The strain rate of the test should also be defined but this is usually neglected because for steels there is only a 10% increase in the flow stress with an order of magnitude change in strain rate (Knott, 1981). Sharp yield points are not observed in stress–strain curves of bainite so it is usual to specify the yield strength in terms of a proof stress. The proof-stress to UTS ratio increases as dislocation motion becomes more difficult at lower temperatures, typically from about $0.67 \rightarrow 0.80$ over the range $300 \rightarrow 70$ K (Krishnadev and Ghosh, 1979).

It is desirable in high-strength steels to have a proof-stress to UTS ratio, r_1, which is less than about 0.8. This helps to ensure that there is substantial plastic deformation prior to ductile fracture. A small value of r_1 in many cases correlates with good fatigue resistance. The disadvantage is that the value of the stress that can be used in design is reduced. Unfortunately, many bainitic steels have r_1 values much lower than 0.8 even though the UTS may be large (Irvine and Pickering, 1965). The internal strains caused by the displacive transformation and the resultant mobile dislocations ensure a low proof stress. Tempering of bainite at 400 °C has only a minor effect on the microstructure but its recovery raises r_1.

The gradual yielding behaviour sometimes persists after stress-relief heat-treatments. The microstructure of bainite is heterogeneous, with fine carbide particles which concentrate stress and hence lead to gradual yielding. There is also a variety of obstacles to dislocation motion, (solute atoms, precipitates

[13:38 3/9/01 C:/3B2 Templates/keith/3750 BAINITE.605/3750-012.3d] Ref: 0000 Auth: Title: Chapter 00 Page: 293 285-342

of different sizes, boundaries), each with a different ability to obstruct plastic deformation. Many of the obstacles are not uniformly distributed so there will exist obstacle-free areas into which dislocations can penetrate at low stresses, thus giving rise to a gradual deviation from elastic deformation (Kettunen and Kocks, 1972; Kettunen and Lepistö, 1976).[†] Another scale of heterogeneity can arise when a large fraction of a phase harder or softer than bainite is included in the microstructure (Hehemann *et al*., 1957). Plastic deformation at first focuses in the softer phase whose yield strength is effectively reduced (Tomota *et al*., 1976). The hard phase only begins to deform when the softer phase has strain hardened sufficiently to transfer load. Small values of r_1 for so-called bainitic steels can frequently be explained by the presence of martensite, or retained austenite in the predominantly bainitic microstructure (Coldren *et al*., 1969). In particular, bainitic steels with austenite yield gradually and hence fail to meet some established industrial specifications which are based on steels with sharp yield points. The specifications need to be modernised to take into account the deformation

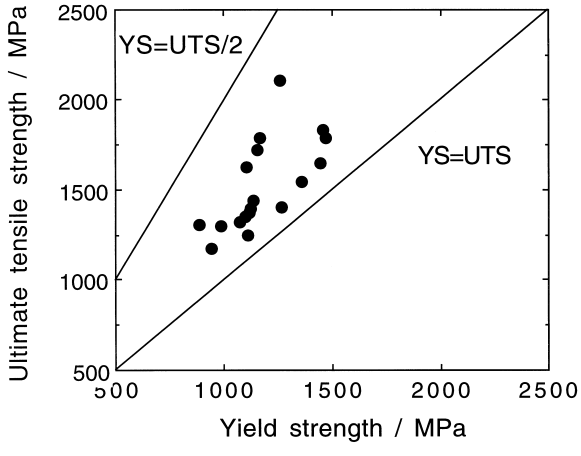

Fig. 12.5 The relationship between the ultimate tensile strength (UTS) and yield strength (YS) in steels with a mixed microstructure of bainitic ferrite, carbon-enriched retained austenite and some martensite.

[†]The deformation behaviour of a microstructure as complex as that of bainite is qualitatively consistent with the statistical theory of slip (Kocks, 1966). In this, a crystal is assumed to contain a random distribution of obstacles of differing strength. Dislocations have a finite probability of overcoming obstacles even when the applied stress σ is below the macroscopic yield stress σ_y. The mean free slip area A_s for dislocation glide varies with σ/σ_y and when dislocations can sweep right across the specimen, $\sigma = \sigma_y$.

behaviour of such steels, which strain harden rapidly and hence meet the ultimate strength requirements with ease. There is direct evidence that low values of r_1 correlate with large amounts of retained austenite in the microstructure, Fig. 12.5 (Sandvik and Nevalainen, 1981).

Retained austenite can in part be transformed into martensite by refrigeration in liquid nitrogen, or by tempering the steel to form ferrite and carbides. The reduction in retained austenite content leads to an increase in yield strength after both of these thermal treatments. The ultimate tensile strength is hardly affected, because the retained austenite in any case decomposes by stress-induced martensitic transformation during the early stages of deformation in a tensile test (Kalish *et al*., 1965).

Gradual yielding is advantageous in forming operations where it helps to avoid 'stretcher strains'. These represent Luders fronts between yielded and unyielded metal. Dual-phase steels are designed to take advantage of the gradual yielding associated with mechanically heterogeneous microstructures. They consist of mixtures of soft proeutectoid ferrite and a hard phase which may be bainite, martensite or indeed, a mixture of three phases.

However, it has been found that intercritically annealed steels containing allotriomorphic ferrite and bainite produced by isothermal transformation can cause discontinuous yielding behaviour because the ferrite strain ages at the temperature where bainite forms (Choi *et al*., 1988). The ageing occurs because of the difference in the solubility of interstitials, between the intercritical annealing temperature and the bainite transformation temperature. It may therefore be possible to avoid quench ageing by generating the required microstructure using continuous cooling heat treatment, thus allowing the interstitials to equilibrate during cooling.

Choi *et al*. have also shown that discontinuous yielding can be avoided if the hard phase is a mixture of bainite and martensite. This is because the latter forms during cooling from the isothermal transformation temperature and generates fresh interstitial-free dislocations allowing the gradual yielding behaviour to be recovered.

Bainitic dual phase steels are weaker than those containing martensite and they have a large r_1 ratio. But they have the advantage of better formability and fatigue strength (Sudo *et al*., 1982, 1983). It follows that r_1 is not always a reliable indicator of fatigue performance.

The required magnitude of the proof-stress/UTS ratio must be assessed for each application. For pipe-line alloys which are low-carbon bainitic steels, used for the conveyance of oil or gas under pressure, the fabricated pipe is hydrotested prior to service. This involves pressurisation to 125% of the planned operating pressure. If the value of r_1 is too low, there is a possibility of gross plastic deformation with failure during hydrotesting. It is common therefore to specify a minimum value of r_1 which is in the range 0.85–0.90 (Jones and

Johnson, 1983). On the other hand, steel columns used in the construction of buildings in earthquake areas are required to absorb energy without failure; a low r_1 value is then an advantage.

12.4 Ductility

It was noticed as early as 1957 by Irvine and Pickering, that low-carbon bainitic or martensitic steels always show superior tensile ductility when compared with their high-carbon counterparts, even when the comparison is made at identical strength. Their subsequent work (1965) confirmed that ductility can be improved by reducing the carbon concentration of a fully bainitic microstructure while maintaining its strength using substitutional solid solution strengthening.

Ductile fracture in good quality commercial steels which do not contain many nonmetallic inclusions propagates via the nucleation, growth and coalescence of voids. Macroscopic fracture occurs when the voids link on a large enough scale. If the number density of voids is large, then their mean separation is reduced and coalescence occurs rapidly, giving very little plastic deformation before fracture, i.e. a small overall ductility (Fig. 12.6). The number of carbide particles per unit volume increases with the carbon concentration of

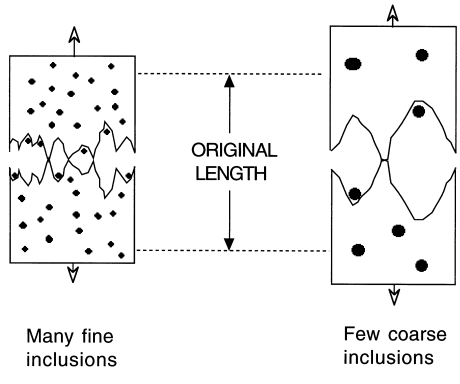

Fig. 12.6 An illustration of how a large density of void nucleating particles can result in fracture with a low overall ductility, even though the material fails by gross plastic deformation on a microscopic scale.

[†]The term *clean* implies the absence of nonmetallic inclusions of a size larger than cementite particles. High-carbon steels, where the cementite particle size may be expected to be large, can be air-melted, and yet be classified as clean. For low-carbon bainitic steels, significant differences in toughness are obtained for the air-melted and vacuum-refined conditions (McEvily and Magee, 1968), so that only the latter can be considered clean.

bainitic steels (Pickering, 1958). It is these carbides which are responsible for void nucleation in clean steels, so it follows that ductility must decrease with increasing carbon concentration even if the strength remains constant or decreases (Bhadeshia and Edmonds, 1983a,b).[†]

In steels which do not transform completely to bainite, ductile void formation initiates at the hard regions of untempered martensite which result from transformation of carbon-enriched residual austenite (McCutcheon *et al*., 1976). Presumably, the brittle failure of martensite provides the nuclei for void growth. This is why the elongation of fully bainitic low-carbon steels is always better than that of tempered martensite of the same strength, whereas the situation reverses when the comparison is made at high carbon concentrations (Irvine and Pickering, 1965). It is more difficult to obtain fully bainitic microstructures free from untempered martensite when the carbon concentration is large.

The linking of voids is associated with internal necking between adjacent voids. Since the necking instability depends on the rate of work hardening, the ductility should decrease if the work hardening rate is small. Experimental results do not bear this out. Deep and Williams (1975) have shown that tempered upper bainite strain hardens more rapidly than tempered lower bainite. And yet, the two microstructures have identical ductilities even when the interparticle spacing and mean carbide size are kept constant. Thus, the effect of work hardening, and indeed of the yield stress, on the ductile failure of bainitic steels is not yet understood.

The tensile elongation of fully bainitic, low-carbon steels is better than that of quenched and tempered martensitic steels of equivalent strength but the reverse is true at high carbon concentrations (Irvine and Pickering, 1965). The reduction of area is, on the other hand, always worse for bainitic steels. These results are not easily explained. Ductility trends as indicated by elongation data are inconsistent with reduction of area measurements. Martensitic steels almost always have larger reductions of area in tensile tests against comparable bainitic steels.

12.4.1 Ductility: The Role of Retained Austenite

Both the total elongation, and its uniform component, reach a maximum as a function of the fraction of retained austenite, when the latter is varied by altering the degree of isothermal transformation to bainitic ferrite (Sandvik and Nevalainen, 1981). The difference between the uniform and total elongation decreases as an optimum volume of retained austenite is reached. Further increases in retained austenite content are associated with tensile failure which occurs before the necking instability, in which case the difference between uniform and total elongation vanishes.

The best elongation behaviour is observed when the retained austenite is present mainly in the form of films between the sub-units of bainite, rather than as blocky regions between the sheaves of bainite (Sandvik and Nevalainen, 1981). The optimum austenite content increases as the transformation temperature decreases; this is because a finer microstructure incorporates more of the austenite in film form for a given fraction of bainite. For the same reason, elongation becomes less sensitive to retained austenite content as the transformation temperature is reduced. While mechanically unstable austenite causes a reduction in toughness for bainitic steels (Horn and Ritchie, 1978; Bhadeshia and Edmonds, 1983a,b), the ductility improves via the TRIP effect because of lower strain rates involved in measuring elongation.

It must be emphasised that all these results have yet to be interpreted quantitatively. Changes in retained austenite content cannot easily be made without altering other factors such as the tensile strength and the distribution of the austenite. For example, Miihkinen and Edmonds (1987b) have reported a monotonic increase in the uniform and total ductility with retained austenite content. The latter was varied by altering the transformation temperature, so that the strength increased as the austenite content decreased.

12.5 Impact Toughness

The concept of toughness as a measure of the energy absorbed during fracture is well-developed. It is often measured using notched-bar impact tests of which the most common is the Charpy test. A square section notched bar is fractured under specified conditions and the energy absorbed during fracture is taken as a measure of toughness. The notch is blunt; it concentrates stress thereby increasing plastic constraint, making brittle fracture more likely. The tests are conducted over a range of temperatures, and a plot of the impact toughness versus temperature is called an impact transition curve, which has a sigmoidal shape (Fig. 12.7a). The flat region of the curve at high temperatures is the *upper shelf* which represents ductile failure. The corresponding flat region at lower temperatures is called the *lower shelf* and represents cleavage failure. In between these is the transition region with mixed cleavage and ductile fracture. The impact transition temperature (T_t) is usually defined that at which the fracture surface shows 50% cleavage fracture.

The Charpy test is empirical in that the data cannot be used directly in engineering design. It does not provide the most searching mechanical conditions. The sample has a notch, but this is less than the atomically sharp brittle crack. Although the test involves impact loading, there is a requirement to start a brittle crack from rest at the tip of the notch, suggesting that the test is optimistic in its comparison against a propagating brittle crack (Cottrell,

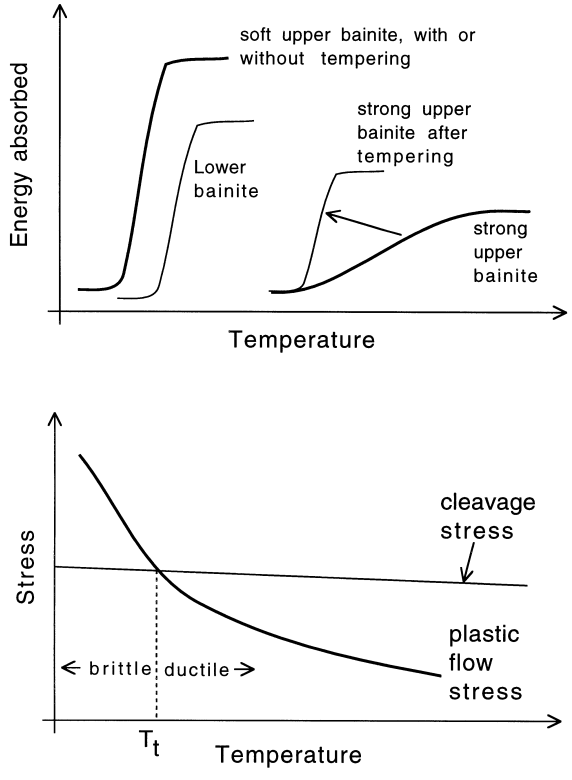

Fig. 12.7 Schematic illustration of impact transition curves (a) and of the cause of the ductile/brittle transition temperature (b) in body-centred cubic metals where the plastic flow stress is much more sensitive to temperature than the cleavage stress.

1995). Most materials can be assumed to contain sub-critical cracks so that the initiation of a crack seems seldom to be an issue.

The Charpy test is nevertheless a vital quality control measure which is specified widely in international standards, and in the ranking of samples in research and development exercises. It is the most common first assessment of toughness and in this sense has a proven record of reliability. The test is usually carried out at a variety of temperatures in order to characterise the ductile–brittle transition intrinsic to body-centred cubic metals with their large Peierls barriers to dislocation motion. In such metals, the cleavage stress is insensitive to temperature, the stress required for plastic flow rises rapidly as the temperature decreases (Fig. 12.7b). The increase in plastic flow stress is partly a consequence of the large Peierls barrier but also because of the

[13:38 3/9/01 C:/3B2 Templates/keith/3750 BAINITE.605/3750-012.3d] Ref: 0000 Auth: Title: Chapter 00 Page: 299 285-342

ubiquitous presence of traces of interstitial elements which interact strongly with dislocation motion.

The curves representing the cleavage and flow stress cross at the transition temperature, on a plot of stress versus temperature. Below T_t, cleavage is easier than plastic flow and vice versa. Any effect which raises the plastic yield stress (such as constraint caused by a notch) without influencing the nucleation or growth of cleavage cracks inevitably leads to an increase in T_t. Cleavage fracture is fast, occurs with little warning, absorbs minimal energy and is undesirable; a low transition temperature is therefore an important aim in safe design.

12.5.1 Fully Bainitic Structures

Irvine and Pickering (1963) conducted a major study of the Charpy impact properties of normalised low-carbon bainitic steels (typical composition Fe–0.003B–0.5Mn–0.5Mo–0.1C wt%). Their results are important and simple to interpret because the samples studied were free from proeutectoid ferrite and almost free of martensite.[†]

The impact properties of soft upper bainite were found not to be sensitive to tempering at temperatures as high as 925 K for 1 hr, as long as the ferrite retained its plate shape. After all, the upper bainite was obtained by transformation at high temperatures where tempering occurs during transformation, so that imposed tempering has only minor further effects on the microstructure.

When strong upper bainite is obtained by transformation at lower temperatures, T_t increases but the upper shelf energy decreases. The ductile–brittle transition becomes less well-defined, the region of the impact curve between the upper and lower shelves extends over a larger temperature range (Fig. 12.7a). This temperature range becomes narrower, and T_t and σ_y decrease, on tempering. The larger sensitivity to tempering is consistent with the lower degree of autotempering expected in bainite generated by transformation at low temperatures.

Even higher strength can be obtained by transforming to lower bainite, which surprisingly has good toughness, comparable to the low strength upper bainite. This is because carbide particles in lower bainite are much finer than in upper bainite. Cementite is brittle and cracks under the influence of the stresses generated by dislocation pile-ups (Hahn *et al.*, 1959). The crack may then propagate into the ferrite under appropriate conditions of stress and temperature. The cracks from fine cementite particles are smaller and hence

[†]It is the combination of low carbon and low substitutional solute concentration, the ease of cementite precipitation in these steels, and the continuous cooling heat treatment which allow the bainite reaction to consume all of the austenite.

more difficult to propagate into ferrite, which is the reason for the higher toughness of lower bainite when compared with upper bainite.

Consider a microcrack nucleus as a through thickness Griffith crack of length c. The cleavage stress σ_F is given (McMahon and Cohen, 1965) by:

$$\sigma_F = \left[\frac{4E\sigma_p}{\pi(1-\nu^2)c}\right]^{\frac{1}{2}} \tag{12.2}$$

where E is the Young's Modulus of ferrite, ν is its Poisson's ratio and σ_p is the plastic work of fracture per unit area of crack surface, an effective surface energy. If c is now set equal to the carbide particle thickness c_o, then the fracture stress is found to vary as $c_o^{-\frac{1}{2}}$. The details of this relationship must of course vary with the shape of carbide particles but the general relationship between σ_F and c remains the same; for example, when considering mixtures of ferrite and spheroidal carbides, the stress σ_F necessary to propagate cleavage fracture through the ferrite has been shown to be given by (Curry and Knott, 1978):

$$\sigma_F = \left[\frac{\pi E\sigma_p}{(1-\nu^2)c_d}\right]^{\frac{1}{2}} \tag{12.3}$$

where c_d is the diameter of the penny-shaped crack resulting from the cleavage of the spheroidal carbide particle.

The identification of the crack length c with the carbide particle thickness c_o is a vital assumption which can be justified experimentally for mild steels containing a microstructure of equiaxed ferrite and cementite particles. This is a carbide-controlled fracture mechanism, but the alternative possibility is a grain-size controlled fracture mechanism, in which the fracture stress is that required to propagate cleavage across grains. The parameter c must then be identified with a grain size dimension, and in the case of bainite, with a packet size. Brozzo *et al*. (1977) have demonstrated that for low-carbon bainitic steels (containing 0.025–0.50 C wt%) the covariant bainite packet size is the microstructural unit controlling cleavage resistance. It is nevertheless possible that the carbide size controls the cleavage fracture of high-carbon bainitic steels.

12.6 Fracture Mechanics Approach to Toughness

Most bainitic steels are used in high-strength applications and failure is not usually accompanied by a large amount of plasticity; they are in this sense 'brittle' materials. It is therefore a good approximation to use elasticity theory to represent the stresses in the vicinity of a sharp crack, even though cleavage crack propagation in metals always involves a degree of plastic deformation at the crack tip. Making the further assumption of *linear* elasticity, we have the

linear-elastic-fracture-mechanics (LEFM) approximation. One definition of a sharp crack is that the inevitable plastic zone at the crack tip is small enough to permit the LEFM approximation.

A fracture mechanics approach is more reliable than impact testing because a toughness value is obtained which is a material property, essentially independent of specimen geometry effects. The pre-cracked test samples and conditions such as the strain rate are similar to the conditions experienced during service. The results can be used quantitatively to predict whether a structure is likely to fail catastrophically under the influence of the design stress. There are excellent books and reviews on the subject but a brief introduction is necessary for an adequate discussion of the work on bainite.

Using LEFM, it is possible to show that when a uniaxial tensile stress σ is applied, the stress σ_r at a distance r ahead of a sharp crack tip is given by

$$\sigma_r = K_I(2\pi r)^{-\frac{1}{2}} \tag{12.4}$$

where K_I is a stress intensification factor in mode I (tensile) loading. K_I is a function of the applied stress σ and of the specimen geometry:

$$K_I = \sigma Y\{c/W\} \tag{12.5}$$

where Y is a compliance function which depends on the crack length c and on the specimen width W. For a body of infinite extent, containing a central through-thickness crack of length $2c$, normal to σ, $Y = (\pi c)^{\frac{1}{2}}$. For brittle materials, K_I at fracture takes a unique *critical* value K_{IC}. The latter is then independent of W or other dimensional variables; it is a material constant which can be used to design against catastrophic failure in service.

12.6.1 Microstructural Interpretation of K_{IC}

In considering the role of microstructure in fracture, it is necessary to distinguish between 'large' and 'small' particles. With small particles, the phenomenon controlling fracture is the propagation of particle-sized microcracks into the surrounding ferrite matrix. For larger particles the cracking of the particle represents the critical event, after which the crack propagates into the matrix and across grain boundaries (Gibson, 1988; Burdekin, 1990). For the most part, high-strength steels such as bainitic or martensitic alloys should, if manufactured properly, lie in the small particle regime, where we shall focus attention.

It is sometimes possible to relate K_{IC} values to microstructural and micromechanistic parameters. It can be argued that the critical value of stress intensity which leads to failure must be associated with corresponding critical values of stress σ_C and distance r_C (Knott and Cottrell, 1963; Knott, 1966; Ritchie *et al*., 1973; Knott, 1981):

[13:38 3/9/01 C:/3B2 Templates/keith/3750 BAINITE.605/3750-012.3d] Ref: 0000 Auth: Title: Chapter 00 Page: 302 285-342

$$K_{IC} = \sigma_C (2\pi r_c)^{\frac{1}{2}} \tag{12.6}$$

where σ_C is usually identified with σ_F (eq. 12.2), the local stress required to propagate a microcrack nucleus. σ_F varies with carbide thickness, or more generally, with the size of the microcrack nuclei resulting from the fracture of a brittle phase in the steel; it is relatively independent of temperature.

The interpretation of the distance r_C is less straightforward. The sample used in a fracture toughness test contains a machined notch, but to make the specimen representative of failure during service, it is fatigue loaded to form a sharp crack which grows slowly from the root of the notch. Fatigue loading is stopped as soon as a uniform crack front is established. The specimen is then ready for toughness testing. The fatigue crack tip is sharp, but not as sharp as the tip of a cleavage crack. It does not therefore propagate when the specimen is tensile loaded for the K_{IC} test. Instead, the stress field extending from the fatigue crack tip causes brittle particles within a distance r_C of the tip to fracture. The resulting microcrack nuclei are atomically sharp and propagate into the matrix if the stress σ_C is exceeded. The cleavage cracks then link up with the original fatigue crack and failure occurs rapidly across the specimen section.

It is emphasised that both r_C and σ_C are for most materials, statistically averaged quantities, since all microstructural features exhibit variations in size, shape and distribution. If the carbide particle size and spatial distribution is bimodal, due perhaps to the presence of a mixture of microstructures, then the K_{IC} values obtained are likely to show much scatter. The stress field extending from the crack tip effectively samples a finite volume and it is the microstructure of that volume which determines toughness. Bowen *et al*. (1986) found that K_{IC} values determined for mixed microstructures of upper and lower bainite (the former containing coarser cementite) exhibited a large degree of scatter when compared with a microstructure of just upper bainite or just martensite.

The microstructural interpretation of K_{IC} evidently requires a knowledge of a local tensile stress and a microstructural distance. This approach has been successful in explaining the toughness of mild steels with a microstructure of ferrite and grain boundary cementite (McMahon and Cohen, 1965; Smith, 1966, Knott, 1981) and to a limited extent of steel weld-deposits which have complex microstructures containing nonmetallic inclusions which initiate failure (Tweed and Knott, 1983; McRobie and Knott, 1985). In some of these cases, the critical microstructural features controlling cleavage fracture resistance have been identified directly, giving faith in the r_C concept.

Difficulties arise when attempts are made to use this approach for clean bainitic or martensitic structures. The carbides particles are so fine as to make a direct identification of r_C impossible. The fracture stress σ_F can never-

theless be measured and if it is shown to be constant, then σ_F itself can be used as a measure of 'toughness' (Bowen *et al*., 1986), although it is not clear how possible variations in r_C can be accounted for. A constant σ_F indicates that the critical step in the fracture process is the propagation of a microcrack.

Bowen *et al*. used this approach, together with K_{IC} studies to explain the toughness of tempered martensite and bainite in a low-alloy steel. In all cases, K_{IC} values were found to increase with the test temperature over the range 77–300 K. For the same temperature range, the proof stress decreased with increasing temperature. For a given proof stress, the toughness of bainite was always lower than that of tempered martensite (Fig. 12.8). The fracture stress σ_F was in all cases found to be independent of test temperature, but bainite had a lower σ_F than martensite. The results were explained in terms

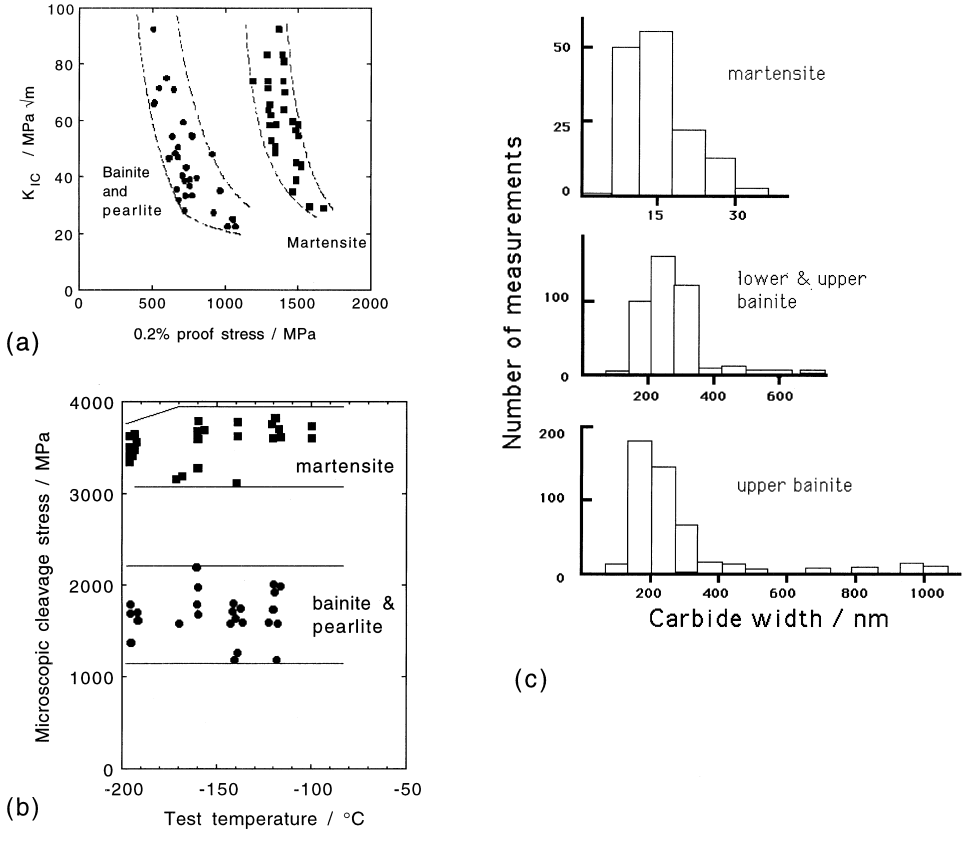

Fig 12.8 (a) K_{IC} values plotted against corresponding values of the 0.2% proof stress. (b) σ_F values plotted against test temperatures. (c) Carbide size distributions obtained from martensitic and bainitic microstructures (after Bowen *et al*.).

of measured cementite particle size distributions (Fig. 12.8). They showed that it is not the mean carbide particle size which determines toughness, but the coarsest particles to be found in the microstructure. A plot of σ_F versus the reciprocal square root of the coarsest carbide thickness gave a straight line as predicted by the modified Griffith equation (eq. 12.2); deviations from this equation occurred at small particle sizes. On this basis, for a given proof stress, the toughness is expected (and found) to increase in the order upper bainite, lower bainite and tempered martensite. Trends like this are also important in the design of welding processes and materials, and there are many qualitative results which confirm that the toughness increases in that order for microstructures in the heat affected zones of steel welds (Inagaki and Hiroyuki, 1984; Harrison and Farrar, 1989).

The reason why the modified Griffith equation fails at small particle sizes is not clear but it means that σ_F becomes relatively insensitive to carbide thickness when the latter is less than about 450 nm.

It must not be assumed that these results spell doom for bainitic microstructures; they need not always have poor toughness relative to tempered martensite. The size of bainitic carbides can be controlled using suitable alloying additions. Indeed, the carbides can be eliminated completely by adding sufficient Si or Al to the steel. The results are valid only for clean steels in which the fracture mechanism is carbide-nucleated and growth-controlled. That the coarseness of carbides controls the toughness of bainite in clean steels is emphasised by the observation that lower bainite with its finer carbides and higher strength nevertheless has a better toughness than the softer upper bainite. All other things being equal, toughness is expected to improve as the strength is reduced, making plastic deformation easy.

The micromechanistic model for the toughness of bainite contains the terms σ_C and r_C, the former defining the stress to propagate a microcrack in a cementite particle, and the latter the distance over which the stress is large enough to cause carbide cracking. The distance r_C is expected to be small in comparison with the width of a bainite sheaf, so the toughness of bainite or martensite should not be dependent on the austenite grain size or the bainite packet size. This prediction has been demonstrated to be the case for tempered martensite (Bowen *et al*.) but contradictory results exist for bainite. Naylor and Krahe (1974) using notched-bar impact tests have shown that a refinement in the bainite packet size leads to an improvement in toughness. The impact transition temperature of bainitic steels is also found to decrease as the austenite grain size decreases (Fig. 12.9), although this might be because the packet size becomes finer at small austenite grain sizes. The austenite grain size in Irvine and Pickering's experiments was varied by controlling the temperature at which hot-rolling finished, or by reheating into the austenite phase field, before the steel was continuously cooled to bainite.

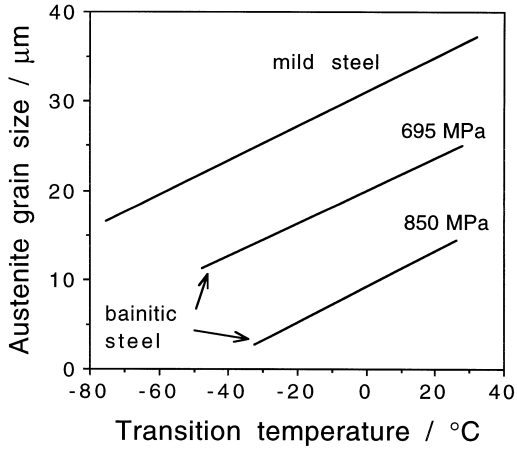

Fig. 12.9 Variation in the impact transition temperature as a function of the austenite grain size (after Irvine and Pickering, 1963).

The fracture stress σ_F and the critical distance r_C do not vary much with temperature, although K_{IC} for bainite is found experimentally to increase as the test temperature rises. This apparent contradiction arises because of the LEFM approximation. In practice, the effect of temperature is to reduce the yield strength. The size of the plastic zone at the crack tip increases so that more work is done as the crack propagates, leading to an increase in K_{IC} (Ritchie *et al.*, 1973).

Finally, it is worth noting that the austenite grain size cannot always be varied independently. Some carbides may not dissolve if the required grain size is achieved using a low austenitising temperature; these carbides can be detrimental to toughness (Tom, 1973). As the solubility of the carbides increases with austenitising temperature, so does the average carbon concentration in the austenite; more of the austenite is therefore retained to ambient temperature after partial transformation to martensite or bainite (Mendiratta *et al.*, 1972; Kar *et al.*, 1979). Variations in austenite grain size also influence hardenability; a fine grain structure can be detrimental if it causes the formation of transformation products such as allotriomorphic ferrite during cooling of a high strength steel (Parker and Zackay, 1975).

12.6.2 Cleavage Fracture Path

Microstructural observations have demonstrated that during cleavage failure, the cracks propagate undeviated across individual packets of bainite (Pickering, 1967).[†] Similar results have been reported for weld deposits,

where cleavage has been shown to propagate undeflected across packets of bainite, reinitiating only at packet boundaries (Chandel *et al*., 1985). The size of cleavage facets obtained by brittle fracture correlates well with the width of the packets (Naylor and Krahe, 1974), although there are also many results which indicate that the undeflected crack path is some 1.5 times larger than the width of bainite packets (Ohmori *et al*., 1974; Brozzo *et al*., 1977). The larger size of the crack path is because even though adjacent packets of bainite are different crystallographic variants of the orientation relationship, there is a high probability that their cleavage planes are fairly parallel (Brozzo *et al*., 1977). The cleavage crack path can lie on {1 1 0}, {1 0 0}, {1 1 2} or {1 2 3} ferrite planes (Naylor and Krahe, 1975).

The correlation between the cleavage facet size and packet size are for low-carbon, low-alloy steels where the fraction of bainitic ferrite that forms is large and that of cementite, martensite or retained austenite, small. The platelets of ferrite within a packet of bainite therefore touch each other at low misorientation boundaries over large areas, thus giving the crystallographic continuity essential for undeviated cleavage crack propagation. In richly-alloyed steels, the intervening layers of retained austenite may hinder the crack as it passes through a packet. It has yet to be established as to how this effect manifests in the context of a fracture path.

12.7 Temper Embrittlement

There are three kinds of embrittlement phenomena associated with quenched and tempered steels, each of which leads either to a minimum in the toughness as a function of tempering temperature, or to a reduction in the rate at which the toughness improves as the tempering temperature is increased:

12.7.1 650 °C Reversible Temper Embrittlement

Tempering at temperatures around 650 °C promotes the segregation of impurity elements such as phosphorous to the prior austenite grain boundaries, leading to intergranular failure along these boundaries. The reversibility arises because the impurity atmospheres at the grain boundaries can be evaporated by increasing the tempering temperature. Quenching from the higher temperature avoids the resegregation of impurities during cooling, thus eliminating embrittlement.

[†]The terms *packet* and *sheaf* are used interchangeably. The former is conventional terminology in mechanical property studies.

In fact, one of the tests for the susceptibility of bainitic microstructures to impurity-controlled embrittlement involves a comparison of the toughness of samples which are water quenched from a high tempering temperature (680 °C) with those cooled slowly to promote impurity segregation (Bodnar *et al*., 1989).

Studies of creep resistant bainitic steels show that phosphorus and tin, and to a lesser extent manganese and silicon, are all embrittling elements (Bodnar *et al*., 1989). Manganese is known to reduce intergranular fracture strength (Grabke *et al*., 1987). Silicon, on the other hand, enhances the segregation of phosphorus to the austenite grain boundaries (Smith, 1980), and can itself cosegregate with nickel to the grain surfaces (Olefjord, 1978). There are also smaller effects due to arsenic, antimony and sulphur. The tendency for embrittlement correlates strongly with an empirical 'J' factor:

$$J = Mn + Si + 10^4(P + Sn) \tag{12.7}$$

where the concentrations of elements are in weight percent Fig. 12.10.

To summarise, the impurity-controlled temper embrittlement occurs in bainite as it does in martensite; after all, neither of these transformation products cross austenite grain surfaces and hence leave them open for impurity segregation. By comparison, reconstructive transformations products such

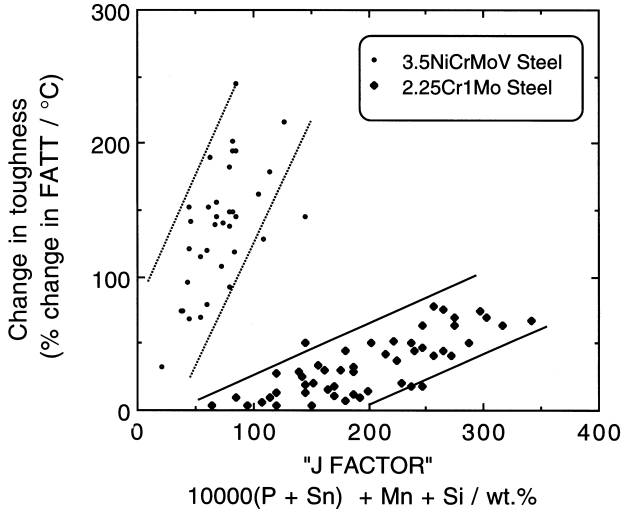

Fig. 12.10 Correlation between the tendency to embrittle and an empirical 'J' factor which is a function of chemical composition (Watanabe and Murakami, 1981; Bodnar *et al*., 1989).

as allotriomorphic ferrite, can grow across and consume the austenite grain surfaces, thereby removing them entirely from the final microstructure.

Finally, it is worth noting that although the science of the embrittlement is well understood, for reasons of cost, commercial steels always contain more impurities than is desirable. Steps must therefore be taken to mitigate the impurity effects, for example by alloying with molybdenum to pin down the phosphorus and prevent it from segregating.

12.7.2 300→350 °C Temper Embrittlement

Fracture is again intergranular with respect to the prior austenite grain boundaries which become decorated with coarse cementite particles during tempering. At the same time, the grain boundaries are weakened by impurity segregation. The cementite particles crack under the influence of an applied stress and in this process concentrate stress at the weakened boundaries. These factors combine to cause embrittlement.

12.7.3 300→350 °C Tempered-Martensite Embrittlement

This effect is common in clean steels, with fracture occurring transgranularly relative to the prior austenite grain boundaries. It is attributed to the formation of cementite particles at the martensite lath boundaries and within the laths. During tempering, the particles coarsen and become large enough to crack, thus providing crack nuclei which may then propagate into the matrix. As a consequence, untempered low-carbon martensitic steels sometimes have a better toughness than when they are tempered, even though the untempered steel is stronger (Fig. 12.11). The cementite behaves like a brittle inclusion.

Both of the impurity-controlled embrittlement phenomena can be minimised by adding about 0.5 wt% molybdenum to the steel. The Mo associates with phosphorus atoms in the lattice thereby reducing mobility and hence the extent to which they segregate to boundaries. Larger concentrations of molybdenum are not useful because precipitation occurs.

In many bainitic microstructures, tempering even at temperatures as high as 550 °C has only a small effect on cementite size and morphology. Consequently, the low-temperature embrittlement phenomena are not found in conventional bainitic microstructures (Ohmori *et al.*, 1974).

When bainite in carbon-containing iron alloys is free from carbides, its microstructure consists of bainitic ferrite, martensite and carbon-enriched retained austenite. In such microstructures, there is a special 'embrittlement' effect associated with the decomposition of the austenite during tempering (Bhadeshia and Edmonds, 1983a,b). The effect is specific to clean steels and is associated with a large reduction in the work of fracture even though the

[13:38 3/9/01 C:/3B2 Templates/keith/3750 BAINITE.605/3750-012.3d] Ref: 0000 Auth: Title: Chapter 00 Page: 309 285-342

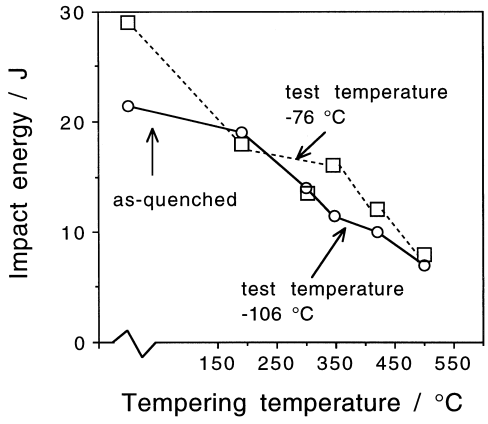

Fig. 12.11 Plot of toughness versus tempering temperature for a high-purity martensitic steel, illustrating that the toughness is reduced even though the strength decreases on tempering (Bhadeshia and Edmonds, 1979b).

failure mode is microscopically ductile. Ductile failure occurs by the nucleation and linkage of microvoids. In the absence of carbide particles, the number of voids nucleated is small, so that the total plastic strain before the voids link is large since they are widely spaced (Fig. 12.6). When the austenite decomposes, the resulting carbides increase the number density of void nucleation sites; the smaller spacing between the voids then reduces the plastic strain to failure, even though the bainite weakens on tempering. The effect is obvious from an examination of fracture surfaces: those from untempered bainite exhibit larger dimples, indicative of widely spaced void nucleation sites (Fig. 12.12). Similar reductions in the ductility and toughness have been correlated versus the decomposition of austenite to carbides in high-silicon bainitic cast irons (Dubensky *et al.*, 1985; Gagne, 1985; Shieh *et al.*, 1993, 1995). Other work has indicated that even the presence of carbides within the lower bainitic ferrite can impair toughness (Miihkinen and Edmonds, 1987c).

12.8 Fatigue Resistance of Bainitic Steels

There are few studies of fatigue phenomena in bainitic steels because they have not had many structural applications when compared with martensitic alloys. Notable exceptions are the creep-resistant alloys used in the power generation industry, where high cycle fatigue is an issue for rotating parts and thermal fatigue resistance becomes important for plant designed to operate intermittently. Fatigue crack propagation in hydrogen-containing environments (chemical or coal conversion plant and pressure vessels) can be life limiting

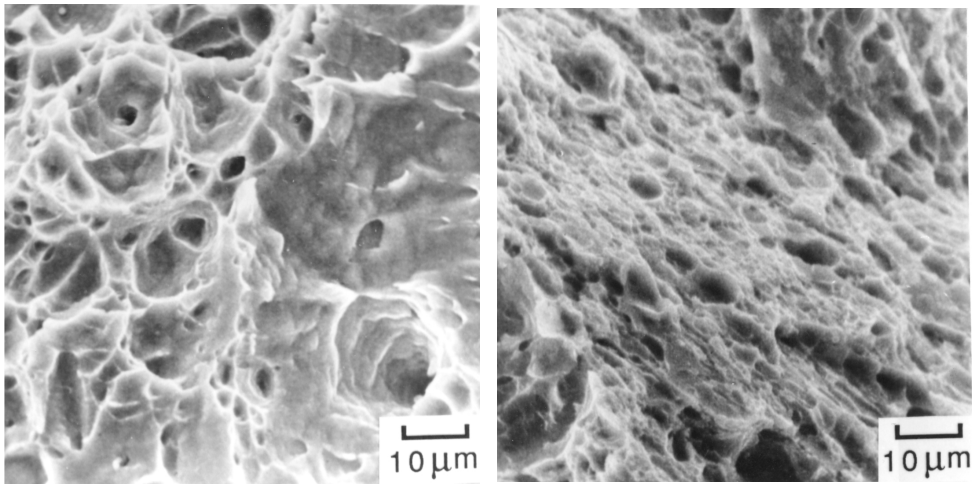

Fig. 12.12 Scanning electron micrographs of the fracture surfaces of untempered (a) and tempered (b) samples, showing the much reduced dimple size in the latter sample which contains numerous carbide particles which help nucleate voids.

and so there are more studies in this area for bainitic alloys. Sub-surface fatigue caused by rolling-contact stresses can similarly limit the life of rails in the transportation industries.

12.8.1 Fatigue of Smooth Samples

Fatigue tests on smooth samples give information on the sensitivity of the specimen to fatigue crack initiation. Such tests are mostly relevant for materials which are clean, i.e. they are free from defects which might propagate under the influence of the applied alternating stress. The results from tests on smooth samples are expressed in the form of an $S-N$ curve, which is a plot of $\ln\{\sigma_a\}$ versus $\ln\{N\}$, where σ_a is the alternating stress amplitude and N the number of cycles to failure (Fig. 12.13).

Materials which strain-age show a *fatigue limit*, which is a value of the alternating stress amplitude below which fatigue failure does not occur. The fatigue limit is the stress below which fatigue cracking never develops, and is usually ascribed to dynamic strain-aging in which the mobile dislocations are pinned by interstitials. Another view is that the limit should be identified with the need for plasticity to spread across grain boundaries for the successful propagation of cracks (Wilson and Oates, 1964; Mintz and Wilson, 1965; Petch, 1990). Fatigue cracks are said not to develop when plasticity is confined to the surface regions of the samples. This alternative interpretation is supported by the fact

[13:38 3/9/01 C:/3B2 Templates/keith/3750 BAINITE.605/3750-012.3d] Ref: 0000 Auth: Title: Chapter 00 Page: 311 285-342

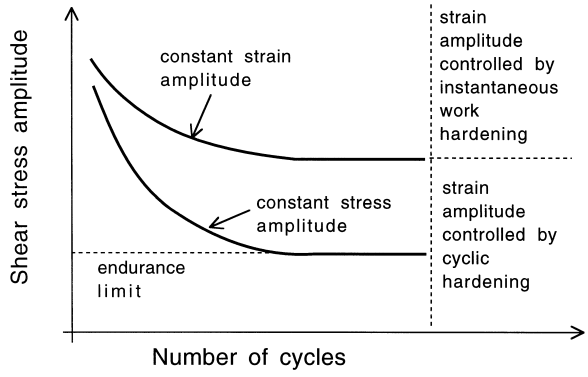

Fig. 12.13 Schematic *S–N* curves for fatigue.

that a fatigue limit can be found even when the test temperature is so low that interstitials can hardly be mobile enough to enable dynamic strain aging. At the same time the role of interstitials is recognised as an additional factor since the fatigue limit actually rises as the temperature is raised to a point where ageing becomes possible (Petch, 1990).

Notice that even smooth samples will have non-uniformities at the surface. These develop into cracks which are small in comparison with the microstructure but they do not grow when the stress amplitude is below the fatigue limit. The cracks are halted by strong microstructural barriers. Chapetti *et al*. (1998) which have defined the nature of the non-propagating crack and of the microstructural feature which acts as a strong barrier, which must be overcome by raising the stress amplitude beyond the fatigue limit (Table 12.1).

Table 12.1 Microstructural observations from smooth specimen fatigue crack growth tests done at stress amplitudes close to the fatigue limit. The non-propagating crack is present at stresses below the fatigue limit but is stopped from advancing by a strong microstructural barrier. After Chapetti *et al.* (1998).

Microstructure	HV	Non-propagating crack	Strong barrier
Ferrite–Pearlite $(\alpha + P)$	127	Across α grain	α/α or α/P grain boundary
Ferrite–Bainite $(\alpha + \alpha_b)$	181	Across α grain	α/α_b boundary
Bainite–Martensite $(\alpha_b + \alpha')$	288	Across packets of laths	Austenite grain boundary

[13:38 3/9/01 C:/3B2 Templates/keith/3750 BAINITE.605/3750-012.3d] Ref: 0000 Auth: Title: Chapter 00 Page: 312 285-342

Mild steels with a microstructure of equiaxed proeutectoid ferrite exhibit a fatigue limit. For other materials, an *endurance limit* is defined as the value of the stress amplitude corresponding to a fatigue life of say $N = 10^8$. It is worth noting that fatigue stresses are in practice less than half the ultimate tensile strength of the steel, so that the plastic strain per cycle can be small.

Fatigue tests on smooth samples can be carried out with the stress amplitude maintained constant for all cycles, or with the plastic strain amplitude fixed for each cycle (Fig. 12.14). The test chosen depends on the nature of the application, but the two kinds of experiments can reveal different information on the relationship between microstructure and fatigue properties. Clearly, when the strain per cycle is a fixed quantity, the alternating stress amplitude needed to maintain the strain increases with the number of cycles as the material fatigue hardens during the test. The hardening eventually reaches a saturation level after many cycles and the stress σ_a does not then vary with N (Fig. 12.14). During each half cycle σ_a has to be raised to the instantaneous flow stress σ_{iy} which can be determined experimentally by interrupting the test at any stage. As the test proceeds, σ_{iy} can be expected to increase as instantaneous work hardening occurs. If σ_s is the value of σ_{iy} at saturation, the ratio $r_2 = \sigma_a/\sigma_s$ is always expected to be close to unity because the applied stress σ_a has to rise to the value of σ_{iy} (Kettunen and Kocks, 1967).

For a test in which the alternating stress amplitude is kept constant, the plastic strain per cycle decreases as the material *cyclically hardens*, until it eventually reaches an approximately constant value. In cyclic hardening, σ_a is constant but σ_{iy} rises, whereas in fatigue hardening $\sigma_a \simeq \sigma_{iy}$ (Kettunen and Kocks, 1972). During the test, σ_{iy} increases due to cyclic hardening as the mean free slip area for dislocations (A_s) decreases. σ_{iy} eventually reaches the saturation value σ_s and at that stage, A_s remains approximately constant with N.

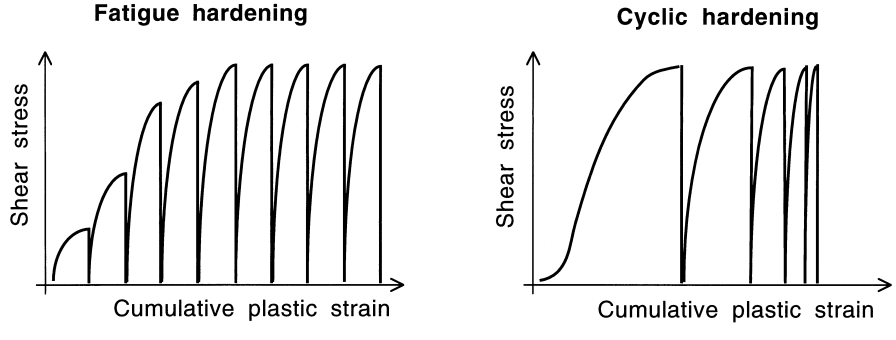

Fig. 12.14 Schematic illustration of constant plastic strain and constant stress fatigue tests (after Kettunen and Kocks, 1967).

[13:38 3/9/01 C:/3B2 Templates/keith/3750 BAINITE.605/3750-012.3d] Ref: 0000 Auth: Title: Chapter 00 Page: 313 285-342

The area A_s at saturation may be larger than the mean slip area per obstacle in which case the to and fro movement of dislocations causes an accumulation of damage which eventually may eventually lead to fatigue failure. However, if A_s is of the order of the mean free slip area per obstacle, because σ_a is low, then the dislocations bow between obstacles, a process which leads to energy dissipation but not to damage accumulation. The applied stress σ_a at which this happens is the endurance limit and fatigue failure does not then occur for many millions of cycles. For cyclic stressing, the ratio r_2 varies with σ_a, but its value corresponding to the endurance limit (i.e. r_e) is predicted to be $\simeq 0.65 - 0.75$ for single crystal specimens (Kocks, 1967). For polycrystalline specimens of lower bainite, $r_e \simeq 0.51 - 0.55$, depending on the way in which the saturation flow stress σ_s is defined. Bainite yields gradually so a saturation *proof* stress has to be substituted for σ_s, and the proof stress has to be measured after an arbitrary (though small) plastic strain. Kettunen and Lepistö (1976) found that the saturation proof stress defined at a strain of 0.02 gives the best agreement with theory. The stress was measured by testing specimens which had first been fatigue cycled to about 20% of their fatigue life to be sure that the specimens are in a state of saturation. It is a good approximation for lower bainite to take $r_2 = (\sigma_a/\sigma_y)$ where σ_y is the proof stress obtained from an ordinary uniaxial tensile test, even though the microstructure is then not in the saturated condition.

Cyclic hardening correlates with the rate of work hardening in monotonic tensile tests. The rate decreases during both fatigue tests and during monotonic tensile testing. The endurance limit can be identified with the onset of a critical (low) value of the rate of work hardening, associated with the approach to saturation in the context discussed above. Since the ultimate tensile strength is also determined by the point at which a reduced rate of hardening cannot keep up with increasing stress due to reduction of area, the endurance limit should correlate well with the UTS, and this is experimentally found to be the case (Kettunen and Kocks, 1967, 1972). This correlation should remain valid as long as the failure mode is ductile.

12.8.2 Fatigue Crack Growth Rate

For many engineering applications, the steels used can be assumed to contain subcritical cracks, in which case the initiation of cracks is not a controlling feature of fatigue life. The lifetime of the component then depends on the rate at which these cracks can grow slowly to a critical size leading to catastrophic failure. If the plastic zone at the crack tip is small when compared with the characteristic dimensions of the specimen, then most of the material surrounding the tip behaves elastically. Linear elastic fracture mechanics can be used to estimate the stress intensity range ΔK felt at the crack tip due to the alternating

stress. The stress intensity range can be related to the crack growth rate da/dN, which is the average distance advanced by the crack front per cycle.

Experiments indicate that there is a minimum threshold value of ΔK below which subcritical cracks do not propagate (Fig. 12.15). For many applications, the majority of fatigue life is spent at near threshold levels of stress intensity since the crack growth rates there can be incredibly small, the average advance of the crack front sometimes being less than an interatomic spacing per cycle. Beyond the threshold regime, the crack growth rate increases with ΔK, until the 'Paris Law' regime is reached (Fig. 12.15) the relationship between the stress intensity range and the crack growth rate is empirically found to be of the form:

$$\frac{da}{dN} = C_4 \Delta K^m \tag{12.8}$$

where C_4 is a constant and m is called the Paris constant.

The crack growth rates in regime A where the stress intensity range is near the threshold value are found to be most sensitive to microstructure, mean stress and environment (Ritchie, 1979). The threshold region is of practical

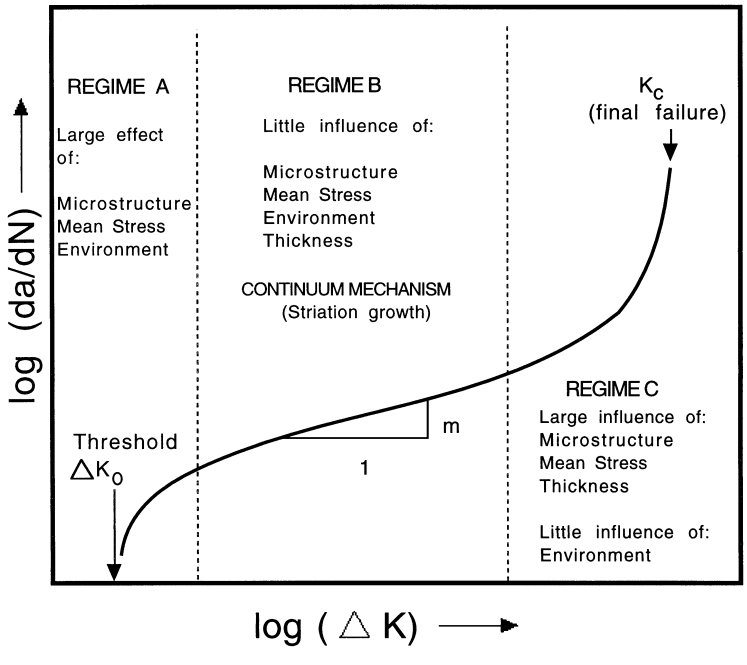

Fig. 12.15 Schematic illustration of the variation in fatigue crack growth rate as a function of the stress intensity range (after Ritchie, 1979.)

[13:38 3/9/01 C:/3B2 Templates/keith/3750 BAINITE.605/3750-012.3d] Ref: 0000 Auth: Title: Chapter 00 Page: 315 285-342

significance because many cracked components spend a good proportion of their fatigue life in that region. The threshold value of ΔK (i.e. ΔK_0) correlates directly with the *cyclic* yield strength (Fig. 12.16) which is in general less than the yield strength as measured in a uniaxial tensile test (Ritchie, 1979). The sensitivity of ΔK_0 to strength decreases as the mean stress amplitude increases.[†] This correlation is expected because the plastic zone at the fatigue crack tip is subject to alternating stresses; cyclic deformation of this kind must be different from monotonic strain hardening. Cyclic softening in quenched and tempered martensitic steels is usually attributed to rearrangements of the dislocation substructure and to a reduction in the dislocation density with alternating load. The softening occurs also because some of the plastic strain is reversible, a phenomenon analogous to the Bauschinger effect.

With some microstructures, the cyclic yield strength is found to be larger than the ordinary yield strength. In lightly tempered martensitic steels, the cyclic hardening is believed to occur due to dynamic strain ageing (Thielen

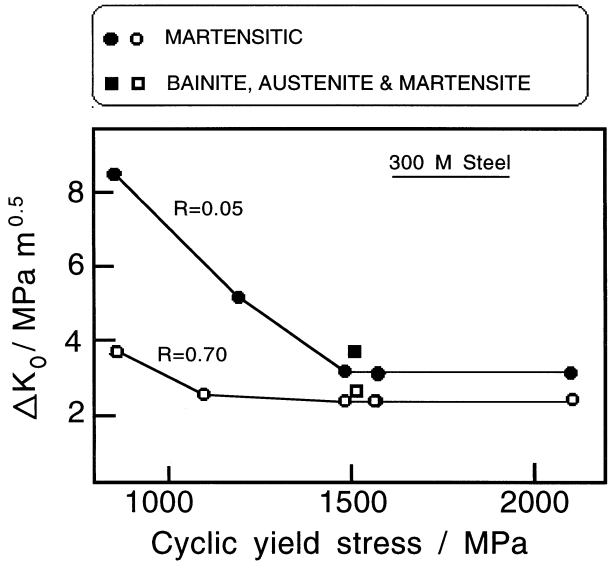

Fig. 12.16 Correlation of the threshold stress intensity range for fatigue crack propagation versus the cyclic yield stress for fully martensitic, and mixed microstructures at two values of R, which is the ratio of the minimum to maximum stress intensity (Ritchie, 1977a).

[†]This behaviour contrasts with the fatigue or endurance limit for steels, which increases with strength since it becomes more difficult to initiate cracks in smooth samples as the strength increases. The threshold value of ΔK on the other hand, depends on the ability of existing long cracks to grow, an ability which is enhanced by an increase in strength.

et al., 1976). For a high strength steel transformed isothermally to a mixed microstructure of bainite, martensite and retained austenite, Ritchie (1977a) found that the deformation-induced transformation of retained austenite to martensite reduced the reversibility of plastic strain during cyclic deformation, causing the cyclic yield strength to exceed the ordinary yield strength and consequently leading to a reduction in ΔK_0 (Fig. 12.17). Later work on metastable austenitic stainless steel has confirmed that fatigue induced martensitic transformation is accompanied by drastic cyclic hardening (Bayerlein *et al.*, 1992).

Cyclic softening therefore improves the near threshold fatigue crack growth resistance as long as the overall tensile strength is not reduced by a modification of the microstructure. Consistent with this, it is found that in a Fe–0.5Cr–0.5Mo–0.25V wt% steel, coarse grained precipitation hardened ferritic microstructures show significantly lower fatigue crack growth rates near ΔK_0, than higher strength bainitic or martensitic microstructures in the same alloy (Benson and Edmonds, 1978). In all cases, the crack path was found to be predominantly transgranular, with the bainite or martensite lath boundaries bearing no obvious relationship with the fracture surface.

A major reason why the threshold region is microstructure sensitive is that at higher stress intensities, the plastic zone size at the crack tip can be many times

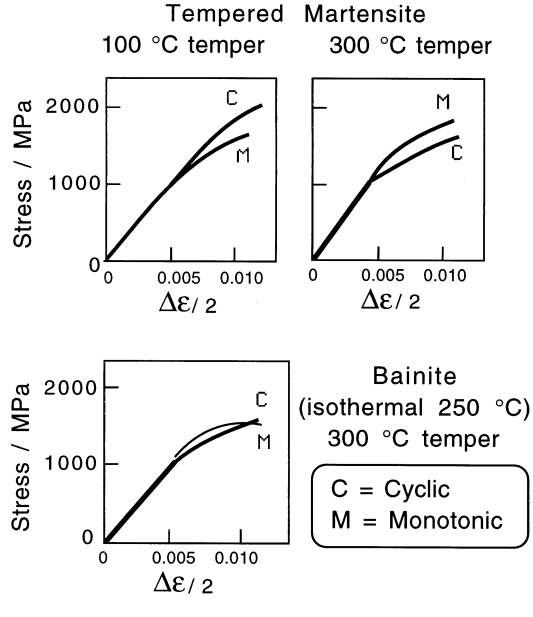

Fig. 12.17 Data illustrating the differences between the cyclic and monotonic yield behaviours for tempered martensite and bainite in 300M steel (Ritchie, 1977a).

[13:38 3/9/01 C:/3B2 Templates/keith/3750 BAINITE.605/3750-012.3d] Ref: 0000 Auth: Title: Chapter 00 Page: 317 285-342

greater than the grain size or other microstructural feature. Benson and Edmonds showed that in the threshold region, the maximum plastic zone size was about 3–5 times the ferrite grain size, and comparable with the austenite grain size in the case of the bainitic and martensitic microstructures (i.e. a few times larger than the lath or packet size).

In the Paris Law regime (regime B, Fig. 12.15), the material behaves essentially as a continuum with little demonstrable influence of microstructure or mean stress. For ductile materials, the crack advances by a striation mechanism although other modes of fracture might occur at the same time in embrittled materials, giving values of m which are much larger than the $m = 2$ value expected theoretically. As the crack continues to grow at increasing ΔK, the maximum stress intensity begins to approach the critical value K_{IC} characteristic of final failure. The growth rate then becomes microstructurally sensitive, the dependency on microstructure reflecting its relationship with toughness. Thus, the austenite associated with bainitic microstructures can be beneficial to fatigue in Regime C (Fig. 12.15). The fracture modes in this regime replicate those found in static fracture, e.g. cleavage or intergranular failure.

12.8.3 Fatigue in Laser-Hardened Samples

Surface layers of steel components can be heat-treated with minimal distortion using lasers. The action of the laser is to swiftly heat a thin surface layer which then cools rapidly by the transfer of heat into the underlying material, a process known as 'self-quenching'. A motivation for surface treatments of this kind is to improve the resistance to fatigue. The microstructure of the surface layer can be martensitic or bainitic depending on the composition and shape of the steel, together with the parameters controlling the laser treatment. The general principles discussed above apply, that the fatigue crack growth rate is insensitive to the microstructure in the Paris law regime, but varies with the microstructure when the stress intensity range is close to the threshold value.

In the threshold regime, Tsay and Lin (1998) have shown that for equivalent hardness, a lower bainitic microstructure has better resistance to cleavage crack propagation than one containing tempered martensite. This is because the latter is more sensitive to grain boundary embrittlement leading to intergranular failure during fatigue at ΔK values as low as $25\,\mathrm{MPa\,m^{\frac{1}{2}}}$. Since the tempering temperature was only $300\,^{\circ}\mathrm{C}$, the weakness of the prior austenite grain boundaries must be associated with coarse cementite particles as discussed in section 12.7. The tendency to form such particles at the prior austenite grain boundaries is reduced for a lower bainitic microstructure since the cementite precipitates during the course of transformation.

It is interesting to note that Tsay and Lin induced the formation of lower bainite during laser treatment by preheating the steel to a temperature of 300 °C, a method used widely in the welding industry.

12.8.4 Fatigue and Retained Austenite

Fatigue cracks propagate as damage is accumulated during the cyclic straining of the material at the crack tip. It is natural to expect metastable austenite in the vicinity of the crack tip to transform into martensite, leading effectively to an increase in the strain hardening rate. A high strain hardening rate leads to more rapid crack propagation (Cottrell, 1965), because the ability of the material to accommodate plastic strain then becomes exhausted more readily. The formation of hard martensite in a ductile matrix also decreases the strain preceding fracture.

It might therefore be concluded that the presence of austenite is not beneficial to the fatigue properties. However, this neglects the work that has to be done by the applied stress to induce martensitic transformation (Chanani *et al*., 1972). Stable austenite might also improve the fatigue properties by increasing the ductility of the microstructure.

Figure 12.18 shows fatigue crack propagation data from two samples of carbide-free bainitic microstructures in which the strength was altered by varying the isothermal transformation temperature. It is seen that the threshold stress-intensity increases and the crack propagation rate decreases, as the fraction of retained austenite increases. This is in spite of the fact that the yield strength of the sample with less austenite is in fact larger[†]

12.8.5 Corrosion Fatigue

There are few corrosion fatigue data available for bainitic microstructures, but it is known that environmental effects can accelerate fatigue cracks via a conjoint action of stress and corrosion. Many of the effects are attributable to hydrogen embrittlement. The fresh fracture surfaces created as the crack propagates are vulnerable to environmental attack, as long as there is sufficient time available for the hydrogen to diffuse into the region ahead of the crack front. Consequently, corrosion fatigue is less detrimental at high frequencies of cyclic loading.

Corrosion during fatigue also leads to a reduction in the threshold stress intensity, below which normal fatigue crack growth does not occur, to a value designated K_{CRIT}. The reduction may be so drastic as to make K_{CRIT} of little use

[†]It is sometimes considered that the crack growth increment per cycle should be inversely proportional to the cyclic yield strength. This is because the crack tip opening displacement will be smaller when the yield strength is large. This is opposite to the behaviour illustrated in Fig. 12.18, providing evidence for the beneficial effect of retained austenite.

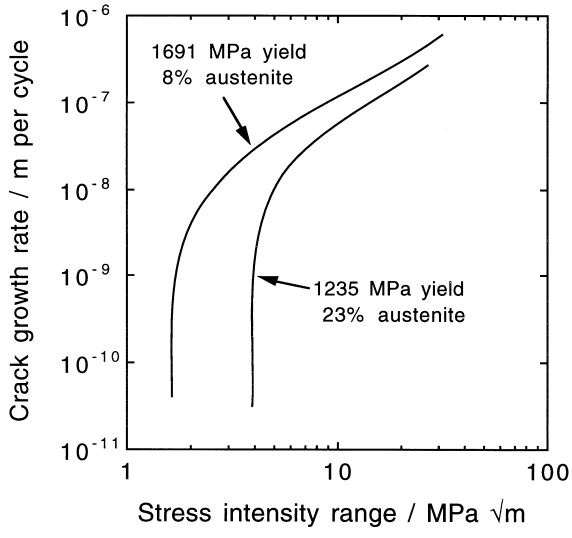

Fig. 12.18 The fatigue crack propagation rate as a function of the stress-intensity range. The chemical composition of the steel is Fe–0.6C–2.3Si–1.5Mn–0.6Cr wt%. The microstructures each consist of a mixture of retained austenite, bainitic ferrite and high-carbon martensite. The high and low yield strength samples are obtained by isothermal transformation at 573 and 643 K respectively (Wenyan *et al.*, 1997).

as a design parameter, since the section sizes necessary to reduce the design stresses to a level at which crack propagation does not occur may be unrealistically large. In such circumstances, the components are assigned service lives calculated using known corrosion fatigue data.

Although it is intuitively reasonable that corrosion should, by chemical degradation, enhance the crack growth rate, there are complications which sometimes lead to an overall reduction in the rate of crack propagation (Dauskardt and Ritchie, 1986). When the stress intensity range and mean stress is low, any corrosion products that form can isolate the crack tip from its environment. Thus, fatigue crack growth in a moist environment occurs at a lower rate than in dry hydrogen (Ritchie *et al.*, 1980; Suresh *et al.*, 1981). Specimens which have been damaged by hydrogen bubble formation prior to fatigue testing can fail more rapidly relative to those in which the bubbles form in the vicinity of the crack front during testing. The expansion associated with bubble formation then induces crack tip closure (Fig. 12.19). All other factors being equal, low strength steels are better at resisting crack growth because plasticity leads to crack tip closure.

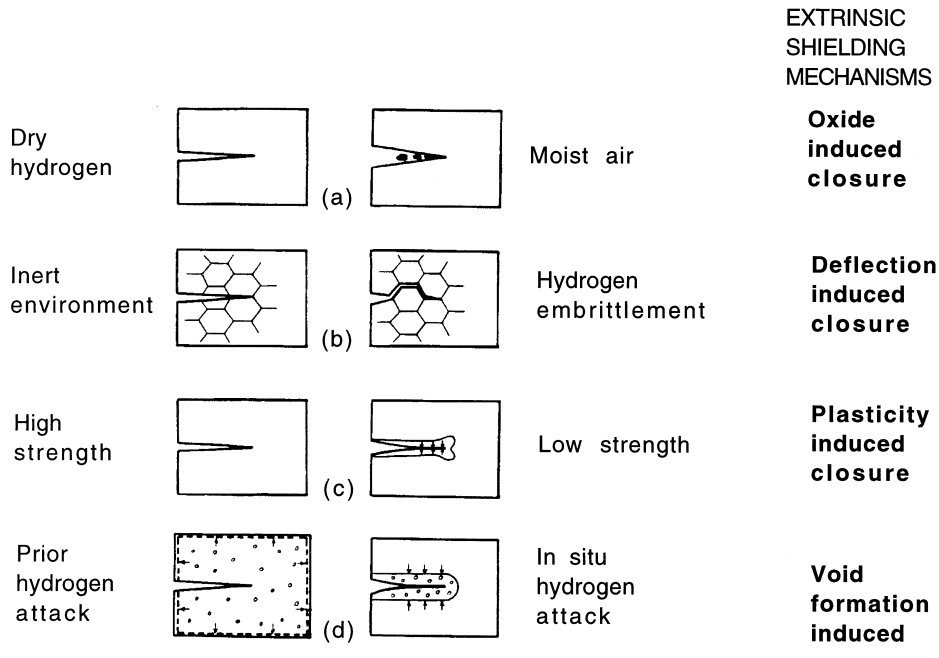

Fig. 12.19 An illustration of the micromechanisms of crack tip shielding, as discussed in the text (Dauskardt and Ritchie, 1986.)

12.8.6 Stress Corrosion Resistance

Cleavage fracture occurs when a critical stress is exceeded over a region ahead of the crack tip, such as to stimulate the growth of an existing microcrack. This critical stress can be reduced by environmental effects. Cleavage fracture then occurs at a critical stress intensity K_{ISCC} which is about a third of K_{IC}. This means that stress corrosion can severely limit the effective use of high strength steels. The effect of corrosion manifests primarily via hydrogen embrittlement, the hydrogen being generated by cathodic reaction at the crack surface. It then diffuses to regions of highest dilatation ahead of the crack tip, leading to a reduction in the cohesive strength (Pfeil, 1926; Troiano, 1960; Oriani and Josephic, 1974).

It is difficult to comment on the relationship of K_{ISCC} with microstructure but it appears that the presence of retained austenite reduces the stress corrosion crack growth rates, by hindering the diffusion of hydrogen to the sites of triaxial tension ahead of the advancing crack front (Parker, 1977; Ritchie *et al.*, 1978). The diffusivity of hydrogen through austenite can be many orders of magnitude smaller than that in ferrite (Shively *et al*. 1966). The permeation of

[13:38 3/9/01 C:/3B2 Templates/keith/3750 BAINITE.605/3750-012.3d] Ref: 0000 Auth: Title: Chapter 00 Page: 321 285-342

hydrogen in high strength steels has been studied using electrochemical techniques (Tsubakino and Harada, 1997). The diffusivity derived from permeation curves is found to be smaller, and the activation energy larger, for steels with retained austenite.

Comparative experiments at constant yield strength, on tempered martensite and on a mixed microstructure of lower bainite, martensite and retained austenite, revealed that the sample containing the greater quantity of austenite exhibited better stress corrosion resistance in a NaCl solution (Ritchie *et al*., 1978). While both samples failed at the prior austenite grain surfaces, the proportion of ductile tearing was greater in the bainitic samples. This was attributed to the ability of retained austenite to act as sinks for impurities thereby reducing segregation to boundaries (Marschall *et al*., 1962). Embrittled boundaries are more susceptible to stress corrosion (Ritchie, 1977b).

These investigations emphasise the role of retained austenite in improving the resistance to stress corrosion, but the conditions under which the austenite is beneficial are limited (Solana *et al*., 1987; Kerr *et al*., 1987). The austenite has to continuously surround the plates of ferrite in order to hinder the diffusion of hydrogen. There are other effects which are more important than that of austenite. Any microstructural modifications which lead to a high density of hydrogen traps (e.g. interfaces between cementite and ferrite) lead to large improvements in stress corrosion resistance.

Kerr *et al*. and Solana *et al*. were able to establish some general principles relating microstructure and stress corrosion resistance (SCR). The sensitivity to microstructure was largest at yield strengths less than about 1000 MPa, and when failure occurred by a transgranular mechanism. Furthermore, the largest improvements obtained did not correlate with the presence of retained austenite. Twinned martensite was deleterious to SCR, presumably because twinned martensite is associated with high carbon concentrations and poor toughness; the twins themselves are innocuous. Mixtures of ferrite and martensite were found to be better, correlating with extensive crack branching due to the high density of interphase interfaces. The presence of lower bainite also led to improved SCR, but the effect could not be separated from any due to the associated drop in yield strength. All other factors being equal, reductions in yield strength correlated strongly with improved SCR (Fig. 12.20). Alloy specific effects were also observed and attributed to differences in the density of hydrogen traps. Indeed, any feature of the microstructure which enables the hydrogen to be dispersed, or which promotes crack branching, improves SCR.

There is recent work using secondary-ion mass spectroscopy on an acicular ferrite microstructure, which suggests that dissolved boron atoms form stable complexes with hydrogen, thereby reducing its mobility (Pokhodnya and Shvachko, 1997).

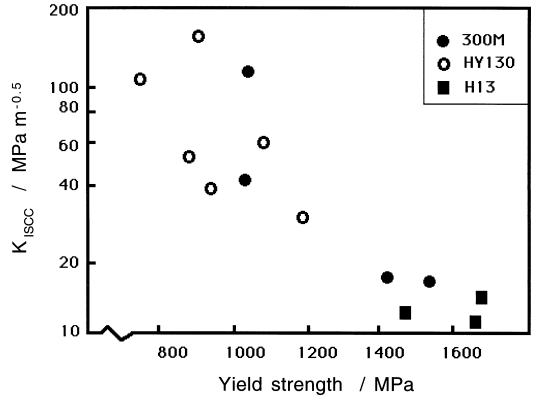

Fig. 12.20 The correlation of stress corrosion cracking resistance versus the yield strength for a variety of steels (Solana *et al.*, 1987)

12.9 The Creep Resistance of Bainitic Steels

Creep-resisting steels used in power plant or in the petrochemical industries are based on low-carbon, low-alloy steels containing chromium, molybdenum, tungsten or vanadium as the significant alloying additions. Low-chromium steels, such as the classical $2\frac{1}{4}$Cr1Mo or 1CrMoV alloys have formed the backbone of the power generation and petrochemical industries for at least five decades, for operating temperatures of 565 °C or less. The $2\frac{1}{4}$Cr1Mo is essentially bainitic, whereas the 9Cr1Mo type alloys developed much later, for higher temperatures and greater corrosion/oxidation resistance, are martensitic. The major applications are in the fabrication of pressure vessels, boiler steam pipes, steam generating and handling equipment, high pressure tubes with thick walls, turbine rotors, superheater tubes, coal to methane conversion plants, petrochemical reactors for the treatment of heavy oils and tar sands bitumen, etc. In addition to creep, they have to be resistant to oxidation and hot-corrosion, sometimes in environments containing hydrogen and sulphur. The pressure vessels in large coal liquefaction and gasification plant may be required to contain mixtures of hydrogen and hydrogen sulphide at pressures up to 20 MPa at 550 °C. The steels have to be weldable and cheap.

Given the demands for service at high temperatures and over 30–50 years, the microstructures must be resistant to other phenomena, such as graphitisation. Protection against graphitisation is one of the reasons why the aluminium concentration is limited to less than 0.015 wt%, and why chromium and molybdenum are used together as alloying additions, because molybdenum on its own promotes the tendency to graphitisation (Hrivnak, 1987). Ambient temperature properties are relevant because the fabricated components must

be safe during periods where elevated temperature operation is interrupted. Fatigue resistance is important to bear in mind but the tolerance to cyclic stresses can frequently be managed by proper engineering design.

The steels might typically be used within the temperature range 480–565 °C, the service stresses being of the order of 15–40 MPa ($\sigma/E \simeq 1\text{–}3\times10^{-4}$). The maximum tolerable creep strain rate is about $3 \times 10^{-11}\,\mathrm{s}^{-1}$. In power plant, the stresses normally originate from a combination of internal steam pressure and the dead weight of the components in large assemblies. The most important property requirement is creep resistance. A greater creep strength can be exploited to reduce the component wall thickness; the resulting reduction in weight allows the support structures to be reduced in scale. It is often the case that the hoop stresses generated by the pressurised steam can be comparable to those due to the weight of the steam pipes, providing the incentive for weight reduction. Higher alloy steels can be used without additional expense, if they have a higher creep strength. Welding also becomes simpler and cheaper for smaller section sizes. Thermal stresses induced by temperature differences between the inner and outer surfaces of any component are smaller with section size, thereby mitigating any thermal fatigue problems associated with the irregular use of the power plant, due for example to variations in electricity demand. Such flexibility can make a substantial difference to the economic performance of electricity-generating plant.

Typical chemical compositions of bainitic steels used for their creep resistance the given in the upper half of Table 12.2; those listed in the lower half represent are corresponding martensitic steels presented for comparison. The newer steels tend to contain less manganese in order reduce their susceptibility to temper embrittlement and banding due to chemical segregation. The hardenability is maintained at reduced manganese concentrations by the overall increase in the concentration of other elements, for example chromium.

The actual chemical composition can in practice vary significantly from the typical value. The specified composition range is generally not tight from a metallurgical point of view (Table 12.2). Indeed, the American Society for Testing Materials has at least twelve standards for the $2\frac{1}{4}$Cr1Mo steel for different applications (Lundin *et al.*, 1986). It is unfortunate that many publications refer only to the nominal designation, and sometimes do not even mention the carbon concentration of the steel concerned. It is now recognised that very small and apparently innocuous variations in chemical composition can explain large variations in the mechanical properties of creep-resistant steels (Kimura *et al.*, 1997).

An interesting reason for keeping the carbon concentration as low as possible, is that it is often necessary to join these steels to stainless steels. There is then a carbon chemical potential gradient which exists at the junction,

Table 12.2 Compositions (wt%) of creep-resistant steels with typical specification ranges. The upper and lower sections of the table represent bainitic and martensitic steels respectively. The sulphur concentration is usually within the range 0.005–0.02 wt%, and that of phosphorus within the range 0.005–0.025 wt%

Designation	C	Si	Mn	Ni	Mo	Cr	V	Others
0.25CrMoV	0.15	0.25	0.50	0.05	0.50	0.30	0.25	–
range	<0.18	0.10–0.60	0.40–0.65	–	0.45–0.65	0.25–0.35	0.20–0.30	–
1Cr MoV	0.25	0.25	0.75	0.70	1.00	1.10	0.35	–
range	0.24–0.31	0.17–0.27	0.74–0.81	0.60–0.76	0.65–1.08	0.98–1.15	0.27–0.36	–
2.25Cr1Mo	0.15	0.25	0.50	0.10	1.00	2.30	0.00	–
range	<0.16	<0.05	0.3–0.6	–	0.9–1.1	2.0–2.5	–	–
Mod. 2.25Cr1Mo	0.1	0.05	0.5	0.16	1.00	2.30	0.25	Ti = 0.03 B = 0.0024
3.0Cr1.5Mo	0.1	0.2	1.0	0.1	1.5	3.0	0.1	–
range	<0.16	<0.5	0.30–0.60	–	0.45–0.65	4.0–6.0	–	–
3.5NiCrMoV	0.24	0.01	0.20	3.50	0.45	1.70	0.10	–
range	<0.29	<0.11	0.20–0.60	3.25–4.00	0.25–0.60	1.25–2.00	0.05–0.15	
9Cr1Mo	0.10	0.60	0.40	–	1.00	9.00	–	–
range	<0.15	0.25–1.00	0.30–0.60	–	0.90–1.10	8.00–10.00	–	–
Mod. 9Cr1Mo	0.1	0.35	0.40	0.05	0.95	8.75	0.22	Nb = 0.08 N = 0.05
range	0.08–0.12	0.20–0.50	0.30–0.60	<0.2	0.85–1.05	8.00–9.50	0.18–0.25	Nb 0.06–0.10 N 0.03–0.07 Al <0.04
$9Cr\frac{1}{2}MoWV$	0.11	0.04	0.45	0.05	0.50	9.00	0.20	W = 1.84 Nb = 0.07 N = 0.05
range	0.06–0.13	<0.50	0.30–0.60	<0.40	0.30–0.60	8.00–9.50	0.15–0.25	Nb 0.03–0.10 N 0.03–0.09 Al <0.04
12CrMoV	0.20	0.25	0.50	0.50	1.00	11.25	0.30	–
range	0.17–0.23	<0.5	<1.00	0.30–0.80	0.80–1.20	10.00–12.50	0.25–0.35	–
12CrMoVW	0.20	0.25	0.50	0.50	1.00	11.25	0.30	W = 0.35
range	0.17–0.23	<0.5	<1.00	0.30–0.80	0.80–1.20	10.00–12.50	0.25–0.35	W <0.70
12CrMoVNb	0.15	0.20	0.80	0.75	0.55	11.50	0.28	Nb 0.30 N 0.06

causing it to migrate during service at high temperatures (Fig. 12.21). The migration occurs from the low-alloy to the high-alloy steel, causing a decarburised layer to develop in the former and an intense region of carbide precipitation in the latter. The overall integrity of the joint is therefore jeopardised (Klueh, 1974a; Lundin *et al.*, 1982). Naturally, a reduced carbon concentration also leads to inferior creep properties given that the steels rely on alloy carbides for their resistance to creep so that a compromise is necessary (Klueh, 1974a,b).

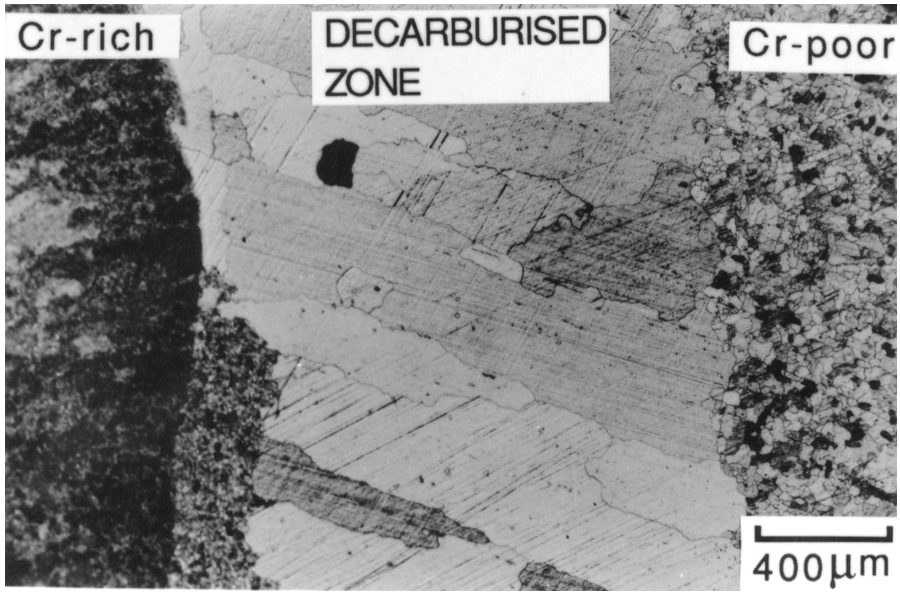

Fig. 12.21 Optical micrograph of a junction between mild steel and a $2\frac{1}{4}$Cr1Mo alloy, showing the development of a decarburised zone in the mild steel side of the joint after tempering (Race, 1990).

The standard alloys sometimes contain trace additions of boron and titanium, added presumably to enhance the bainitic hardenability in the manner discussed in Chapter 6. Unintentional trace impurities such as tin and antimony are also known to have disproportionate effects on creep strength for reasons which are not well understood (Collins, 1989). The alloys are usually fabricated by welding, and the filler material used can be chemically different from the parent plate; the CrMoV steels are usually welded with $2\frac{1}{4}$Cr1Mo fillers in order to ensure good creep properties in the weld metal.

12.9.1 Heat Treatment

For power plant applications, the steels are usually air cooled ('normalised') after austenitisation. The component thickness may vary from 12–120 mm; the thickness determines the heat treatment time in order to allow the component to achieve uniform temperature. On the other hand, heat flow analysis shows that the specified periods are excessive and could in principle be reduced (Greenwell, 1989). The temperature to which the steels are heated for austenitisation is usually about 100 °C above the Ae_3 temperature, or 50 °C above the Ac_3 temperature when the heating rate is about 1 °C per minute. Lower temperatures lead to correspondingly smaller austenite grain sizes,

[13:38 3/9/01 C:/3B2 Templates/keith/3750 BAINITE.605/3750-012.3d] Ref: 0000 Auth: Title: Chapter 00 Page: 326 285-342

which can be beneficial to mechanical properties. The creep mechanism in service is not controlled by grain boundary diffusion or sliding, but rather by the motion of dislocations past precipitates.

Given that it is impossible to achieve uniform cooling in large components, it is reasonable to expect variations in the microstructure and mechanical properties as a function of position. For a typical range of chemical compositions encountered within the $2\frac{1}{4}$Cr1Mo designation, the normalised microstructures consist of mixtures of allotriomorphic ferrite and bainite, with the fraction of bainite in the range 0.34–0.94 (Murphy and Branch, 1971). The effect on the mechanical properties due to these variations is pronounced during the early stages of service, but the differences in creep strength vanish over the long term.

After normalisation, the steels are given a stress-relief treatment by tempering at 660–700 °C for some 2–14 h, depending on application and component size. This not only produces the required microstructure containing relatively stable carbides, but also mitigates residual stresses arising from welding operations. These heat treatments are so severe that the precipitates are in an overaged condition (Pilling and Ridley, 1982).

12.9.2 $2\frac{1}{4}$Cr1Mo Type Steels

This is a popular steel which has been used reliably for many decades. Its creep resistance, like that of many low-alloy steels used in the power generation industry, comes from fine and stable dispersions of alloy carbides together with contributions from solid solution strengthening. The latter is especially important in the long term when the carbide dispersions have become ineffective due to coarsening. Molybdenum is particularly effective as a solid solution strengthening element (Lundin *et al*., 1982, 1986). The alloy design should be such as to avoid tying up all of the molybdenum in the form of carbides. The carbon concentration should therefore be controlled carefully to achieve the best compromise between the need for carbides and solution strengthening. Typical values of the creep rupture strength of $2\frac{1}{4}$Cr1Mo steel are illustrated in Fig. 12.22.

Investigations have shown that the ferrite/bainite microstructure in $2\frac{1}{4}$Cr1Mo steel is stronger in creep than martensite because M_2C, which is replaced eventually by more stable carbides during service, persists for shorter times in a martensitic microstructure (Baker and Nutting, 1959; Murphy and Branch, 1971). M_2C is more stable in ferrite when compared with bainite or martensite. These observations have yet to be explained.

12.9.3 1CrMoV Type Steels

These steels have been used in the manufacture of rotors for steam turbine power generating plant. 1CrMoV steels are austenitised at temperatures within

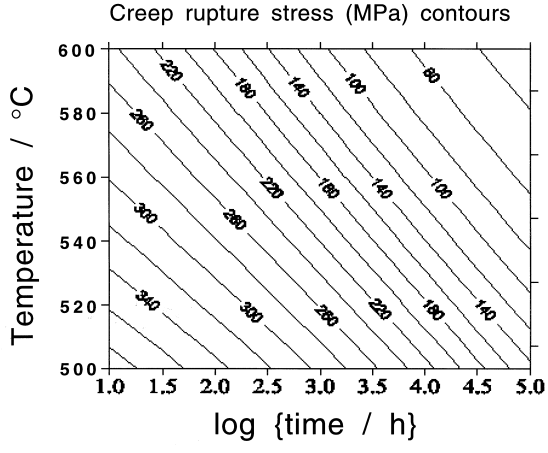

Fig. 12.22 Creep rupture strength of $2\frac{1}{4}$Cr1Mo steel as a function of temperature and time.

the range 950–1000 °C for 1–14 h and air cooled or furnace cooled to give a fully bainitic or a mixed microstructure of ferrite and bainite (Myers *et al*., 1968; Murphy and Branch, 1969; Strang *et al*., 1994). Tempering is in the range 690–710 °C for time periods up to 20 h. The resulting microstructure is a fine dispersion of V_4C_3 particles (about $\simeq 12$ nm size) in a matrix of ferrite.[†] Other carbides such as M_3C and $M_{23}C_6$ may also form when the carbon concentration is in excess of that required to react with the vanadium. These other carbides are coarse and precipitate mainly at the prior-austenite or ferrite grain boundaries.

The alloy is martensitic in the quenched condition; tempering at 690 °C for 20 h converts the martensite into ferrite containing V_4C_3 but for some unknown reason the carbide particles are much coarser with a typical size of 50 nm (Buchi *et al*., 1965; Myers *et al*., 1968). The creep strength of 1CrMoV steels in the tempered bainite condition is higher than in a tempered martensitic state, but this may not be due to the finer carbides in the tempered bainite. The observed activation free energy for creep is inconsistent with a process controlled by the climb of dislocations; the spacing between particles is too close to allow dislocation bowing (Myers *et al*., 1968). It is suggested that it is the interaction of dissolved vanadium with dislocations which controls creep deformation. The finer carbides in the tempered bainite leave a larger concentration of dissolved vanadium since the solubility of solute increases with interface curvature via the Gibbs–Thompson capillarity effect. The greater

[†]The V_4C_3 precipitates contain some iron, manganese molybdenum and chromium in solid solution, although vanadium is by far the major carbide-forming constituent (Senior, 1988).

concentration of soluble vanadium is claimed to be responsible for the better creep strength of tempered bainite. The interaction of vanadium atoms with dislocations must be important, but so must the dispersions of particles since it is unlikely that Fe–V solid solutions would have good creep properties in their own right.

The uniformity of the V_4C_3 dispersion depends on the form of M_3C present (Buchi *et al*., 1965). If the vanadium and carbon concentrations are stoichiometrically balanced, then M_3C is eliminated during tempering and the V_4C_3 dispersion is uniform. Otherwise, the regions around M_3C particles are found to be free from V_4C_3. Since the M_3C particles are mostly located at prior austenite or ferrite grain boundaries, V_4C_3-free zones form at the boundaries. This results in poor creep properties (Buchi *et al*., 1965; Murphy and Branch, 1969).

12.9.4 $\frac{1}{4}$CrMoV Type Steels

$\frac{1}{4}$CrMoV steels have a low hardenability so they are used with microstructure of allotriomorphic ferrite and a small fraction of pearlite. Fine V_4C_3 dispersions form on tempering. These steels have a higher creep ductility than the 1CrMoV alloys at a slightly lower creep strength. The lower creep ductility of 1CrMoV steels is because creep cavitation occurs at both the ferrite/ferrite and ferrite/bainite boundaries, whereas the $\frac{1}{4}$CrMoV cavitates mainly at the ferrite/pearlite which are not as susceptible to cavitation (Murphy and Branch, 1969). It is also argued that a larger fraction of ferrite permits a greater relaxation of stresses, thereby inhibiting cavity nucleation and growth (Jones and Pilkington, 1978).

12.9.5 Enhanced Cr–Mo Bainitic Steels

Many attempts have been made to improve on the properties of the low-alloy creep-resistant steels, especially in the context of pressure vessels in hydrogen environments. A higher concentration of alloy carbide-forming elements can reduce the stability of cementite, which is prone to hydrogen problems (Ritchie *et al*., 1984; George *et al*., 1985). Those alloys containing unstable carbides such as cementite and Mo_2C react with ingressed hydrogen, leading to decarburisation, cavitation and to the formation of methane bubbles at interfaces. Damage by hydrogen is thought to occur in three stages (Vagarali and Odette, 1981; Shewmon, 1976). The first stage, during which the microstructure and macroscopic mechanical properties are largely unaffected, involves the nucleation and growth of bubbles. This is followed by rapid attack as methane bubbles grow and coalesce into fissures at the grain boundaries, leading to swelling and a deterioration of mechanical properties. The final stage is

[13:38 3/9/01 C:/3B2 Templates/keith/3750 BAINITE.605/3750-012.3d] Ref: 0000 Auth: Title: Chapter 00 Page: 329 285-342

extensive decarburisation with the dissolution of carbides as the system attempts to maintain an equilibrium carbon concentration in the ferrite.

Thick steel plates (300–400 mm) are required in applications such as coal conversion plant. Conventional steels do not have adequate hardenability so attention has been focussed on improving the popular bainitic $2\frac{1}{4}$Cr1Mo steel, with the aim of extending the temperature range over which the alloy can be utilised, whilst maintaining the bainitic microstructure. Modifications include microalloying to improve elevated temperature strength, larger concentrations of chromium for improved resistance to hydrogen embrittlement, carbide stabilising additions such as vanadium and niobium, and nickel, boron and carbon additions for improved bainitic hardenability (Wada and Eldis, 1982; Wada and Cox, 1982, 1984; Ishiguro *et al*., 1982, 1984; Kozasu *et al*., 1984; Parker *et al*., 1984; Klueh and Swindeman, 1986).

Ishiguro *et al*. (1982) developed an alloy which differs from $2\frac{1}{4}$Cr1Mo steel in that it has a negligible silicon concentration, a lower carbon concentration (0.1 wt%) and 0.25V–0.02Ti–0.002B wt%. It is designated the 'Modified $2\frac{1}{4}$Cr1Mo' steel, with improved creep strength, impact toughness and resistance to temper embrittlement. The titanium combines with nitrogen, so that the boron can remain in solution and increase hardenability; boron otherwise forms a nitride which is less stable than that of titanium. The creep strength is improved because of vanadium carbides which make the bainitic microstructure more resistant to tempering (Klueh and Swindeman, 1986).

An alloy which has received a lot of attention has the chemical composition Fe–3Cr–1.5Mo–0.1V–1Mn–0.1C wt% developed by Wada and coworkers (1982, 1984). After austenitisation at about 1000 °C for two hours and air cooling, it has a microstructure which is essentially a mixture of bainitic ferrite and austenite/martensite, of the kind normally associated with the $2\frac{1}{4}$Cr1Mo steel discussed earlier. The extra alloying elements add to solution hardening, an important factor determining the long-term creep strength.

An advantage of the higher chromium concentration is that cementite is replaced more rapidly by carbides such as M_7C_3, $M_{23}C_6$ and M_6C, thus rendering the microstructure less susceptible to severe hydrogen attack. Bainite in $2\frac{1}{4}$Cr1Mo steel is far more sensitive to a high pressure hydrogen embrittlement than a tempered martensitic microstructure (Chung *et al*., 1982). This is because the carbon-enriched retained austenite associated with bainite decomposes into intense clusters of cementite particles which react with hydrogen. The cementite in tempered martensite is more uniformly distributed. At higher chromium concentrations, for example in the 3.5Cr1Mo bainitic steels, the cementite is quickly replaced by $M_{23}C_6$ making the alloy less sensitive to hydrogen exposure (George *et al*., 1985).

Manganese and silicon contribute to austenite grain boundary embrittlement (Bodnar *et al*., 1989). A bainitic steel in which the concentration of these

elements is minimised is the 3.5Ni3CrMoV alloy which is insensitive to hydrogen and temper embrittlement effects when compared with the $2\frac{1}{4}$Cr1Mo steel (Ritchie *et al*., 1984). The larger concentration of chromium and vanadium leads to the dissolution of cementite during tempering at 700 °C, thereby improving the resistance to hydrogen effects. Hydrogen sometimes reacts with carbon dissolved in ferrite producing gases such as methane, which precipitate as bubbles under conditions of severe hydrogen attack. This is another reason why 3.5Ni3CrMoV steel performs better because the concentration of carbon in the ferrite which is in equilibrium with alloy carbides is reduced.

The nickel in 3.5Ni3CrMoV steel improves toughness; it also increases the hardenability, allowing sections as thick as 0.4 m to transform into fully bainitic microstructures. The reduction in the Ae_3 temperature due to nickel permits the use of lower austenitisation temperatures; the resulting refinement of the austenite grain size is beneficial to toughness. Many other steels with lower nickel concentrations have been investigated and found to possess better properties over the conventional $2\frac{1}{4}$Cr1Mo alloy (Spencer *et al*., 1989).

12.9.6 Tungsten-Strengthened Steels

The heat associated with the welding of steels introduces a heat-affected zone (HAZ) in the solid metal adjacent to the weld; the heating and cooling cycle within this zone may induce undesirable microstructures such as untempered martensite. Post-weld heat treatments are then used to render any martensite in the HAZ harmless. However, this is not practical for large constructions, which also cannot be heated prior to welding in order to avoid the formation of brittle martensite.

A new bainitic steel, known commercially as *HCM2S*, has been developed to address these difficulties (Komai *et al*., 1999; Table 12.3). It is a modification of the $2\frac{1}{4}$Cr1Mo alloy with the molybdenum substituted with tungsten; combined with a reduction in the carbon concentration, this leads to a bainitic microstructure without martensite, allowing welding without pre- or post-weld heat treatment. The maximum hardness obtained for typical cooling rates is

Table 12.3 The chemical composition (wt%) of a tungsten-strengthened creep-resistant steel known commercially as *HCM2S*. The concentration of aluminium refers to that dissolved in the ferrite.

C	Si	Mn	P	S	Cr	Mo	W	V	Nb	N	Al	B
0.05	0.2	0.5	0.015	0.001	2.2	0.1	1.6	0.25	0.05	0.008	0.008	0.004

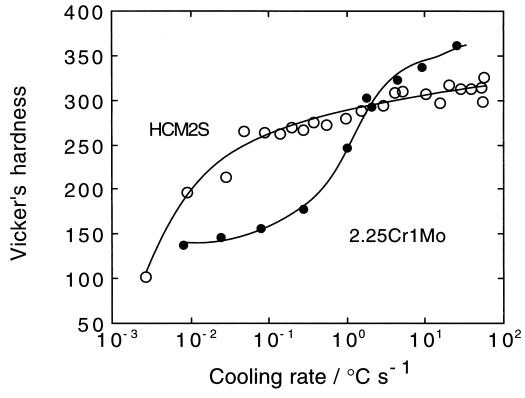

Fig. 12.23 A comparison between the hardness of a tungsten strengthened creep-resistant steel and the classical $2\frac{1}{4}$Cr1Mo alloy. The cooling rate is an average value in the range 800–300 °K s^{-1}. Data from Komai *et al.* (1999).

reduced to about 300 HV which is some 50 HV below that of $2\frac{1}{4}$Cr1Mo steel (Fig. 12.23). The insensitivity of the hardness to the cooling rate is claimed to be desirable in the design of joints.

The microstructure of the steel after normalising is bainite and in the tempered condition consists of tempered bainitic ferrite with cementite, $M_{23}C_6$, and vanadium or niobium carbonitrides. The addition of boron has the effect of stabilising $M_{23}C_6$ and $M_{23}(C,B)_6$ on grain boundaries, thereby retarding dynamic recrystallisation during creep (Miyata *et al.*, 1999). All this makes the alloy creep resistant, so much so that tolerable stress at 600 °C is about twice that of $2\frac{1}{4}$Cr1Mo, and almost matches the more expensive and difficult-to-weld 9Cr1Mo martensitic steels (Fig. 12.24).

The tungsten-strengthened bainitic steel has now performed satisfactorily in service for more than three years. Monitoring tests have shown that the alloy performs better than other steels such as $2\frac{1}{4}$Cr1Mo (Masuyama *et al.*, 1998). Recent work has suggested that a reduction in the manganese concentration can lead to further improvements in the creep strength (Miyatat et al., 1999). This is because M_6C precipitation is slower at low manganese concentrations, thus allowing more tungsten to remain dissolved in, and strengthen the solid solution. A reduction in manganese from 0.5 to 0.01 wt% led to an increase in the creep rupture strength by almost 50 MPa.

12.9.7 Regenerative Heat Treatments

Cavitation and other irreversible creep damage occurs at the late stages in the life of creep-resistant steels. During that period, any loss in properties is due

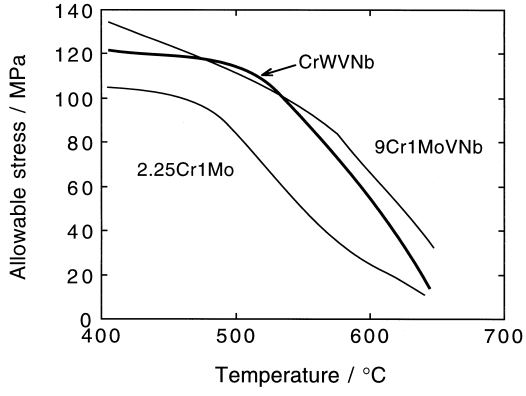

Fig. 12.24 Comparison of the allowable stress, as a function of temperature, for the tungsten-strengthened steel, $2\frac{1}{4}$Cr1Mo and a 9Cr1Mo martensitic steel. After Komai *et al*. (1999).

largely to microstructural changes such as carbide coarsening, changes in the configuration of dislocations, and the general approach of the microstructure towards equilibrium. These microstructural changes can, in principle, be reversed by heating the component back into the austenite phase field and then allowing it to transform back into the original microstructure. However, such a heat treatment involves high temperatures which may not be feasible with large components.

A possible alternative is to regenerate just the carbides, by annealing the steel at a temperature ($\simeq$700 °C) above the service temperature, but below that at which austenite can form (Senior, 1988). Some of the carbides would then dissolve to reprecipitate in a fine form during ageing at a lower temperature, thereby regenerating a semblance of the original microstructure.

12.9.8 Comparison with Martensitic Creep-Resistant Steels

Modern ferritic creep-resistant steels start with a microstructure which is martensitic. On the other hand, the best established steels of this kind rely on allotriomorphic ferrite or bainite as the starting microstructure. It is therefore pertinent to ask why modern heat-resistant steels are based on martensite.

The probable answer to this has little to do with microstructure. Indeed, when compared under identical conditions, the 9Cr1Mo steel is not better in creep than $2\frac{1}{4}$Cr1Mo (Fig. 12.25); it is only when these alloys are modified with elements such as niobium, vanadium, cobalt and tungsten that they begin to outperform the lower alloy steels.

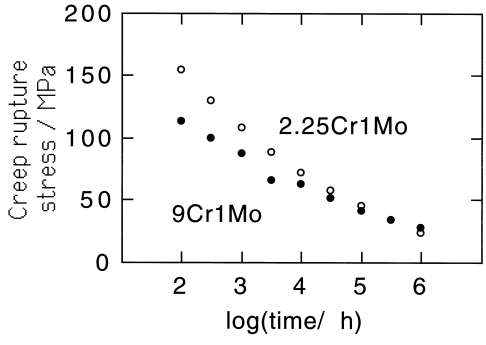

Fig. 12.25 A comparison of the creep rupture strengths of $2\frac{1}{4}$Cr1Mo and 9Cr1Mo steels given identical heat treatments (Bhadeshia, 2000).

The 9Cr1Mo alloys were developed for higher temperatures and greater corrosion/oxidation resistance. A greater chromium concentration is needed to obtain the oxidation and corrosion resistance necessary for higher service temperatures. The chromium must then be balanced by other solutes to avoid an excessive fraction of δ-ferrite. The net solute content then becomes so large that the steels cannot transform to bainite and hence the martensitic microstructure. This is illustrated by the time–temperature transformation diagrams for 2.3, 4.3 and 9.3 wt% chromium steels shown in Fig. 12.26.

It could be argued that a martensitic microstructure, which has a large number density of defects, encourages the precipitation of more numerous and finer carbide particles which are better at resisting creep. Figure 12.27 shows a comparison between bainite and martensite in the same steel; whereas the kinetics of precipitation are not identical in the two cases, the differences are very small over the temperature range of interest (500–650 °C). A martensitic microstructure is not therefore necessary in heat-resistant steels; bainite is adequate.

To summarise, the modern trend towards martensitic creep-resistant steels is associated more with the need to improve the environmental resistance of the alloys rather than microstructural considerations. Indeed, there are well known disadvantages to high hardenability martensitic steels when it comes to weldability.

12.9.9 Transition Metal Joints

It is sometimes necessary in steam turbine assemblies to join the low-alloy ferritic steels to austenitic steels which are more suited for corrosive environments. The joints are usually between tubular elements although thicker joints

[13:38 3/9/01 C:/3B2 Templates/keith/3750 BAINITE.605/3750-012.3d] Ref: 0000 Auth: Title: Chapter 00 Page: 334 285-342

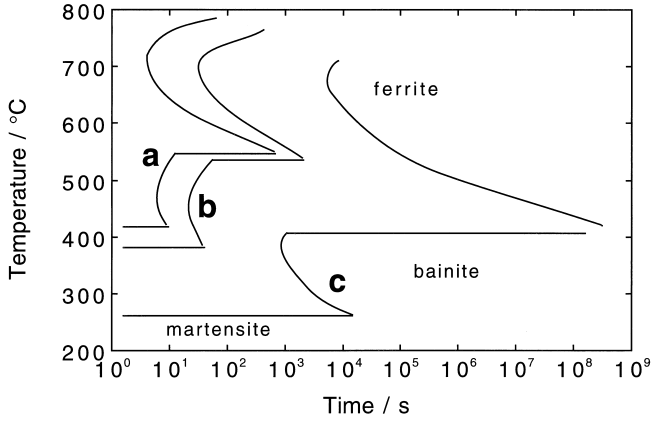

Fig. 12.26 Calculated time-temperature transformation diagrams for steels **x** (0.15C–0.25Si–0.5Mn–1Mo–2.3Cr wt%), **y** (4.3Cr) and **z** (9.3Cr). The transformation curves refer to zero percent reaction. In each case the upper curve represents diffusional transformation whereas the lower curve represents bainite. After Bhadeshia (2000).

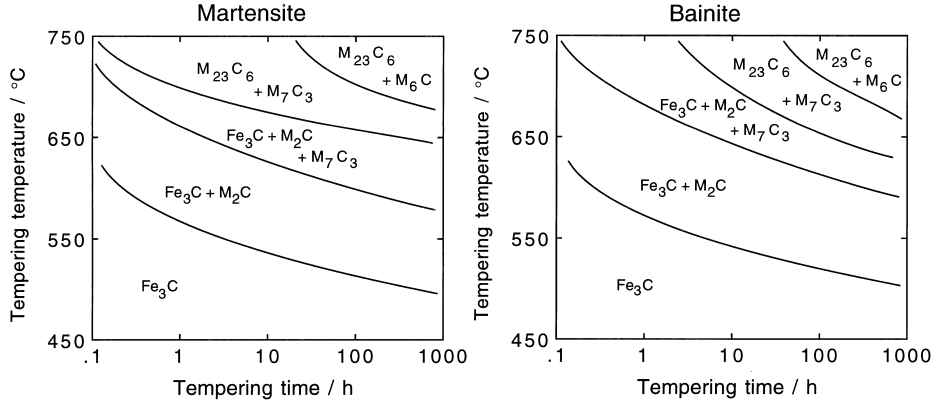

Fig. 12.27 Measured isothermal transformation diagrams for carbide precipitation reactions in $2\frac{1}{4}$Cr1Mo steel: (a) martensitic starting microstructure; (b) bainitic starting microstructure. Adapted from Baker and Nutting (1959).

are occasionally needed. The welds between these dissimilar steels are made using a filler material which is either an austenitic stainless steel, or a nickel-base alloy such as 'Inconel'. The filler material/ferritic steel interface is quite abrupt when the nickel-base filler is used, even though a true metallurgical bond is achieved.

The ferritic steel is usually the $2\frac{1}{4}$Cr1Mo alloy. The chances of a dissimilar metal joint failing during service are large when compared with other welds between like metals. Nath (1982) has suggested that this is because of the complex stresses arising from the different creep properties of the filler, the HAZ and the ferritic base plate. The stresses are such as to intensify creep damage in the vicinity of the weld/base-plate junction.

The microstructure of $2\frac{1}{4}$Cr1Mo is essentially bainite, but after welding, that of the heat-affected zone can contain allotriomorphic ferrite. On the other hand, the coarser austenite grain structure in the HAZ adjacent to the fusion boundary has a higher hardenability and hence transforms into bainite. The allotriomorphic ferrite-containing region which is weak in creep, and is located sandwiched between two stronger regions, the original plate microstructure far away from the weld and the bainite at the fusion boundary. Furthermore, the austenitic (or Inconel) filler material is relatively rigid. This focus-ses the strain in the ferrite, causing the transition joints to fail prematurely. The joints are sometimes heat treated at 700 °C for 30 minutes after welding for stress-relief, but this does lead to a homogenisation of mechanical properties.

Nath (1984) attempted to overcome these problems by reheating the entire welded joint into the austenite phase field at 950 °C for 1 h, followed by air cooling, with the aim of regenerating a fully bainitic microstructure throughout the parent material, including the heat-affected zone. The treatment was successful in improving the creep properties, but the overall performance was still less than that of the unwelded steel. The austenitising heat treatment caused the migration of carbon, which in the case of the ferritic/austenitic joint caused a decarburised zone on the ferrite side of the dissimilar metal interface and a carbon-enriched zone in the austenite on the other side. The carbon migration is driven by the chemical potential gradient resulting from the different chemical compositions of the ferritic and austenitic steels.

12.10 Reduced-Activation Steels

The formation of voids during irradiation with neutrons causes the swelling of metals. Irradiation damage involves the creation of both interstitials and vacancies in equal concentrations, but the former anneal out more rapidly than the latter. The resulting excess concentration of vacancies is relieved by condensation into voids.

Ferrite has a much higher resistance to void swelling than austenite, although nickel base alloys rank alongside the ferritic steels (Little, 1991). Point defects introduced by irradiation condense at *neutral* or *biassed* sinks. The latter are typically dislocations with large Burgers vectors, attracting more interstitials than vacancies. It follows that a large density of neutral sinks enhances the swelling resistance.

It is believed that in ferritic steels, irradiation induces the formation of two kinds of dislocations, one of which is strongly biased whereas the other is neutral. This provides sinks for both interstitials and vacancies, resulting in a smaller excess of void-forming vacancies. There are differences in the void swelling resistance of creep-resistant ferritic steels because of variations in their microstructures. For a given vacancy concentration, a larger number density of vacancy traps leads to a smaller tendency for swelling. Lath boundaries or oxide particles are good vacancy traps.

It is for their swelling resistance that ferritic steels have been considered for structural applications in the construction of the first wall and blanket structures of fusion reactors. But in addition, there is a search for specific alloys whose radioactivity decays most rapidly once they are removed from the radioactive environment. These are the so-called *reduced activation* alloys which have minimal concentrations of Mo, Ni, Nb, Cu and nitrogen, all of which have long-lived radioactive isotopes (Abe *et al*., 1990; Klueh *et al*., 1995). Some of these elements are key constituents of creep-resistant steels, but can be eliminated by using tungsten instead of molybdenum and by substituting vanadium and tantalum for niobium. Some examples of steels which have been studied specifically for their reduced activation are listed in Table 12.4.

Table 12.4 Chemical compositions (wt%) of reduced activation steels (Klueh *et al*., 1995). All of these steels are bainitic with the exception of the 9Cr and 12Cr steels which are martensitic. The chemical compositions of the first group of steels are nominal.

Steel	C	Si	Mn	Cr	V	W	Ta	B
$2\frac{1}{2}$Cr–V	0.1			2.25	0.25			
$2\frac{1}{4}$Cr–1WV	0.1			2.25	0.25	1		
$2\frac{1}{4}$Cr–2W	0.1			2.25		2		
$2\frac{1}{4}$Cr–2WV	0.1			2.25	0.25	2		
Cr–2WV	0.1			5	0.25	2		
9Cr–2WV	0.1			9	0.25	2		
9Cr–2WVTa	0.1			9	0.25	2	0.07	
12Cr–2WV	0.1			12	0.25	2		
$2\frac{1}{4}$Cr–2WVTa	0.1	0.12	0.40	2.41	0.24	2.03	0.05	
$2\frac{1}{4}$Cr–2WVTB	0.090	0.12	0.38	2.37	0.24	2.04		0.005
$2\frac{1}{4}$Cr–2WVTaB	0.093	0.12	0.38	2.36	0.24	2.04	0.05	0.005
2.6Cr–2WVTa	0.11	0.11	0.39	2.59	0.25	2.02	0.05	
2.6Cr–2WVTaB	0.11	0.11	0.39	2.60	0.25	2.07	0.05	0.004
$2\frac{1}{2}$Cr–2W	0.11	0.15	0.39	2.48		1.99		
$2\frac{1}{4}$Cr–2WV	0.11	0.20	0.42	2.41	0.24	1.98		
9Cr–2WVTa	0.10	0.23	0.43	8.72	0.23	2.09	0.07	

Early studies revealed that of the first group of steels listed in Table 12.4, the 9Cr–2WVTa alloy in its martensitic condition has a high strength, good toughness and is able to retain its impact properties after irradiation (Fig. 12.28). On the other hand, the low-chromium bainitic steels do not require a post-weld heat treatment which can be difficult to implement in complex fabricated structures.

Although the high Cr steels show only modest shifts in the ductile-brittle transition temperature following irradiation (Fig. 12.28), difficulties arise when the displacement damage is accompanied by the production of helium by the transmutation of traces of nickel. The helium is insoluble in the matrix and precipitates as small bubbles which embrittle the material. Suppose that the bubble has a radius r, then for an ideal gas the pressure inside the bubble is $P = 2\sigma/r$ where σ is the interface energy per unit area. A small bubble can therefore hold a lot more gas under high-pressure than a large bubble. Typically, a 100 Å bubble holds gas at a pressure of 10^3 atmospheres whereas the pressure is only 1 atmosphere in a bubble which is 10^5 Å in size. Swelling can obviously be minimised by increasing the number density of bubble nucleation sites (Thompson, 1969). Carbide particles are bubble nucleation sites but the high chromium steels form coarse $M_{23}C_6$ particles in contrast to the larger numbers of fine MC or M_2C particles in the lower chromium alloys,

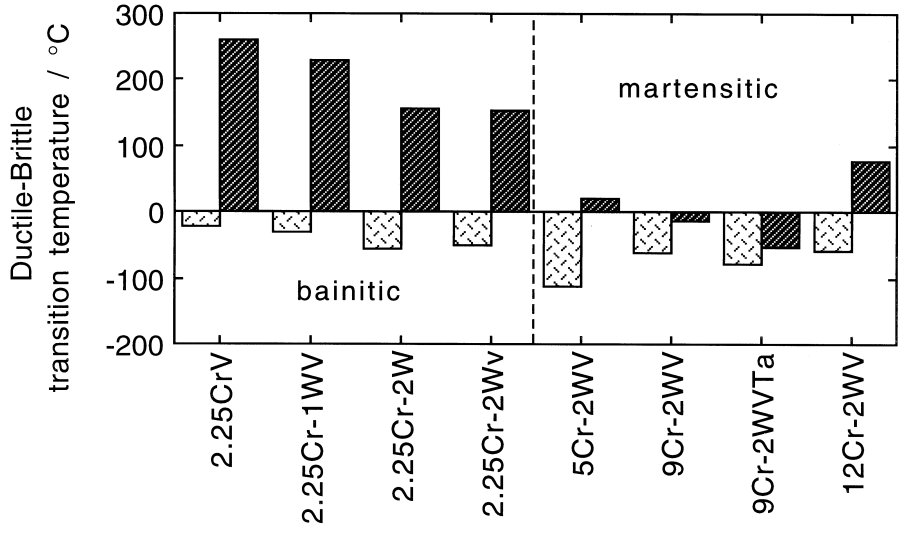

Fig. 12.28 The ductile–brittle transition temperature for normalised and tempered 3 mm diameter bar samples which have been irradiated to about 14 dpa. The 12Cr steel contains some δ-ferrite in addition to martensite. Some of the bainitic steels may also contain allotriomorphic ferrite. After Klueh and Alexander (1999).

making the latter more suitable for fusion reactor applications. On the other hand, the microstructures of the bainitic steels are much more sensitive to the cooling rate from the austenitic condition. Care has to be taken to ensure that the required fine distribution of carbides is obtained in practice.

Some of the steels listed in Table 12.4 are designed with low chromium concentrations to enhance the impact toughness in the irradiated condition. Klueh and co-workers found that the hardenability could be increased with a slight increase in the chromium concentration supported by additions of B and Ta; this resulted in a refined bainitic microstructure with improved toughness and tempering resistance. Indeed, the 2.6Cr–2WVTaB alloy is found to have mechanical properties comparable to those of the best 9Cr steels.

A fine distribution of carbides promotes toughness whether or not the steel is irradiated. The iron carbides which form in the early stages of tempering can be refined by increasing the silicon or aluminium concentration. It is these carbides which set the scene for the subsequent formation of alloy carbides, so there should be a consequential refinement of the entire carbide microstructure. This idea would be worth exploring in the context of reduced-activation steels.

12.11 Steels with Mixed Microstructures

Mixed microstructures consisting of bainite and martensite are usually a consequence of inadequate heat-treatment or the use of steels with insufficient martensitic hardenability.

Early research suggested that bainite in an otherwise martensitic microstructure leads to a deterioration in ductility, toughness and strength (Bailey, 1954; Hehemann *et al*., 1957). The impairment of properties becomes less severe as the bainite forms at lower transformation temperatures, and is related to the difference in strength between martensite and bainite. As this difference decreases, so does the reduction in properties (Hehemann *et al*., 1957).

Tempering homogenises the strength so bainite in a tempered martensite microstructure has less of an effect on the overall properties (Triano and Klinger, 1952; Hehemann *et al*., 1957). For the same reason, a mixture of martensite and lower bainite has better properties than one consisting of upper bainite and martensite. The strength of lower bainite more closely matches that of martensite.

There are, however, circumstances in which mixed microstructures are beneficial. Edwards (1969) observed that after tempering, mixtures of lower bainite and martensite were tougher than either martensite or bainite. There are considerable recent data that following tempering, the presence of bainite in a predominantly martensitic microstructure leads to a higher strength and toughness relative to the single phase samples, Fig. 12.29 (Tomita and

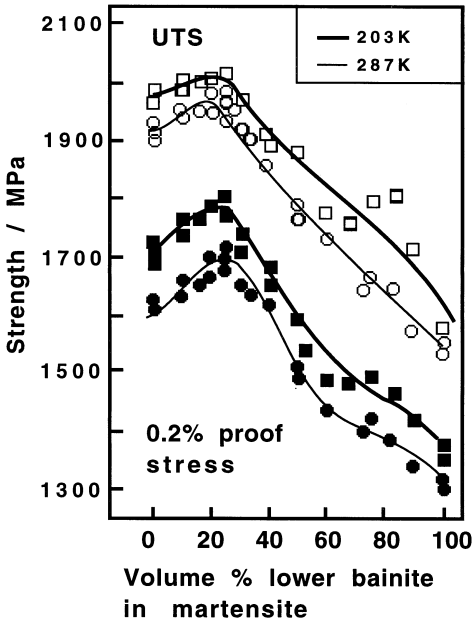

Fig. 12.29 Variation in the 0.2% proof stress as a function of the volume fraction of lower bainite in a mixed, tempered microstructure of lower bainite and martensite. The different curves represent data collected at the temperatures indicated on the diagram.

Okabayashi, 1983a,b 1985a,b, 1987, 1988; Tomita, 1991, 2000). This is because the bainite partitions the austenite, thus refining the size of the martensite packets that form subsequently (Mutui *et al.*, 1977). The refined martensite is stronger, and furthermore, the strength of the bainite is increased by constraint from the strong martensite. But a further point that should be taken into account is that the martensite grows from austenite which is enriched in carbon due to the bainite transformation; it will therefore be expected to be harder.

It is particularly interesting that the strength of a tempered mixture of lower bainite and martensite can exceed that of the martensite alone, and yet can be tougher (Fig. 12.30).

12.12 Summary

The anisotropic, thin-plate shape of bainite ensures that the mean free path for slip is comparable to the plate thickness rather than to the plate length. This means that the major microstructural contribution to strength is via the fine sub-unit size, rather than the sheaf or austenite grain size which are of minor

[13:38 3/9/01 C:/3B2 Templates/keith/3750 BAINITE.605/3750-012.3d] Ref: 0000 Auth: Title: Chapter 00 Page: 340 285-342

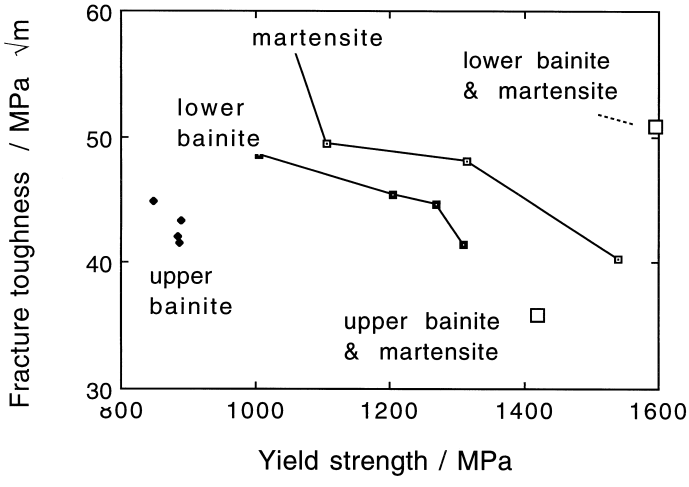

Fig. 12.30 Plot of toughness versus strength for a variety of microstructures in an ultra-high strength steel (data from Tomita, 1988).

importance as far as the strength is concerned. The sub-unit size is so small, that the Hall–Petch relation does not apply; yield is instead controlled by the stress required to expand dislocation loops. This gives a linear relationship between the yield strength and the inverse of the sub-unit size.

Bainitic steels usually exhibit continuous yielding behaviour, with proof stress to UTS ratios which can be much smaller than 0.8. This gradual yielding is a consequence of mobile dislocations, the presence of heterogeneities in the microstructure and residual stresses due to transformation. The ratio can be increased by annealing at low temperatures, although there is not much of a change if the bainite transformation temperature is comparable to the annealing temperature.

There is no doubt that higher carbon concentrations lead to a deterioration of ductility, primarily because of the void nucleating tendency of cementite particles. The presence of large regions of untempered martensite in the microstructure can reduce ductility, whereas retained austenite can in some circumstances enhance it.

The impact toughness of upper bainite deteriorates as its strength increases, but that of lower bainite which has much finer carbides is superior at the same strength level. An interpretation in terms of fracture toughness theory has demonstrated that it is the coarsest carbides in the microstructure which control toughness. Consistent with theory, the fracture strength correlates directly with the reciprocal of the square root of the coarsest carbide size. The scatter in toughness data increases as the microstructure becomes more heterogeneous;

[13:38 3/9/01 C:/3B2 Templates/keith/3750 BAINITE.605/3750-012.3d] Ref: 0000 Auth: Title: Chapter 00 Page: 341 285-342

mixed microstructures of bainite and martensite show greater scatter than fully bainitic samples. During fracture, the cleavage facet dimensions are found to be comparable to those of bainite packets. A refinement of the austenite grain size also reduces the packet size, and consequently leads to an improvement in toughness. All of the impurity controlled temper embrittlement phenomena normally associated with martensite, are found in bainitic steels.

The endurance limit during the fatigue testing of smooth samples correlates well with the UTS of bainitic steels. The threshold stress intensity range for fatigue crack growth is reduced by the presence of retained austenite, because its transformation to martensite prevents the reversal of plastic strain during cyclic deformation. Stable austenite on the whole leads to an improvement in fatigue properties via the ductility it confers to the microstructure.

Retained austenite can lead to an improvement in the stress corrosion cracking resistance, by hindering the diffusion of hydrogen. However, comparable benefits can be achieved by any method which increases the number density of hydrogen traps in the microstructure.

Creep-resistant alloys containing strong carbide-forming elements represent one of the most successful industrial applications of bainitic microstructures. They achieve their creep strength via solid solution strengthening and with the help of fine dispersions of alloy carbides. The most modern of these steels is such that it can be welded without the need for post-weld heat treatments.

Finally, there are now considerable data to suggest that mixed microstructures of bainite and martensite can offer higher strength and toughness than fully martensitic alloys. The mechanism behind this remains to be established.

[13:38 3/9/01 C:/3B2 Templates/keith/3750 BAINITE.605/3750-012.3d] Ref: 0000 Auth: Title: Chapter 00 Page: 342 285-342